NAVAL POSTGRADUATE SCHOOL

MONTEREY, CALIFORNIA

THESIS

CHANNEL ESTIMATION TECHNIQUES FOR SINGLE AND MULTIPLE TRANSMIT ANTENNA ORTHOGONAL FREQUENCY DIVISION MULTIPLEXING (OFDM) SYSTEMS

by

Mumtaz Bilgin Sen

September 2005

Thesis Advisor:	Roberto Cristi
Co-Advisor:	Murali Tummala

Approved for public release; distribution is unlimited

THIS PAGE INTENTIONALLY LEFT BLANK

REPORT DOCUMENTATION PAGE			Form Approved OMB No. 0704-0188
Public reporting burden for this collection of information is estimated to average 1 hour per response, including the time for reviewing instruction, searching existing data sources, gathering and maintaining the data needed, and completing and reviewing the collection of information. Send comments regarding this burden estimate or any other aspect of this collection of information, including suggestions for reducing this burden, to Washington headquarters Services, Directorate for Information Operations and Reports, 1215 Jefferson Davis Highway, Suite 1204, Arlington, VA 22202-4302, and to the Office of Management and Budget, Paperwork Reduction Project (0704-0188) Washington DC 20503.			
1. AGENCY USE ONLY ***(Leave blank)***	**2. REPORT DATE** September 2005	**3. REPORT TYPE AND DATES COVERED** Master's Thesis	
4. TITLE AND SUBTITLE: Channel Estimation Techniques for Single and Multiple Transmit Antenna Orthogonal Frequency Division Multiplexing (OFDM) Systems			**5. FUNDING NUMBERS**
6. AUTHOR(S) Mumtaz Bilgin Sen			
7. PERFORMING ORGANIZATION NAME(S) AND ADDRESS(ES) Naval Postgraduate School Monterey, CA 93943-5000			**8. PERFORMING ORGANIZATION REPORT NUMBER**
9. SPONSORING /MONITORING AGENCY NAME(S) AND ADDRESS(ES) N/A			**10. SPONSORING/MONITORING AGENCY REPORT NUMBER**
11. SUPPLEMENTARY NOTES The views expressed in this thesis are those of the author and do not reflect the official policy or position of the Department of Defense or the U.S. Government.			
12a. DISTRIBUTION / AVAILABILITY STATEMENT Approved for public release; distribution is unlimited			**12b. DISTRIBUTION CODE**
13. ABSTRACT (maximum 200 words) Orthogonal frequency division multiplexing (OFDM) is an efficient multi-carrier modulation technique which can be combined with transmitter and receiver diversity communication systems. Maximal ratio combining (MRC) and space-time block coding (STBC) can be used in conjunction with receiver and transmitter diversity in order to increase the communication system's performance. For these systems, channel estimation and tracking must be performed since the receiver requires channel state information for decoding. In this thesis, block-type and comb-type channel estimation algorithms for OFDM systems over multipath fading channels are studied and simulated. Performance results using simulated frequency-selective channels are presented.			
14. SUBJECT TERMS. Orthogonal Frequency Division Multiplexing (OFDM), Maximal Ratio Combining (MRC), Space Time Block Coding (STBC), Block-Type Channel Estimation, Comb-Type Channel Estimation, Least-Square (LS), Basic Channel Estimation, Simplified Channel Estimation			**15. NUMBER OF PAGES** 93
			16. PRICE CODE
17. SECURITY CLASSIFICATION OF REPORT Unclassified	**18. SECURITY CLASSIFICATION OF THIS PAGE** Unclassified	**19. SECURITY CLASSIFICATION OF ABSTRACT** Unclassified	**20. LIMITATION OF ABSTRACT** UL

NSN 7540-01-280-5500 Standard Form 298 (Rev. 2-89)
Prescribed by ANSI Std. 239-18

THIS PAGE INTENTIONALLY LEFT BLANK

Approved for public release; distribution is unlimited

CHANNEL ESTIMATION TECHNIQUES FOR SINGLE AND MULTIPLE TRANSMIT ANTENNA ORTHOGONAL FREQUENCY DIVISION MULTIPLEXING (OFDM) SYSTEMS

Mumtaz Bilgin Sen
Lieutenant Junior Grade, Turkish Navy
B.S., Turkish Naval Academy, 2001

Submitted in partial fulfillment of the
requirements for the degree of

MASTER OF SCIENCE IN ELECTRICAL ENGINEERING

from the

NAVAL POSTGRADUATE SCHOOL
September 2005

Author: Mumtaz Bilgin Sen

Approved by: Roberto Cristi
Thesis Advisor

Murali Tummala
Co-Advisor

Jeffrey B. Knorr
Chairman, Department of Electrical and Computer Engineering

THIS PAGE INTENTIONALLY LEFT BLANK

ABSTRACT

Orthogonal frequency division multiplexing (OFDM) is an efficient multi-carrier modulation technique which can be combined with transmitter and receiver diversity communication systems. Maximal ratio combining (MRC) and space-time block coding (STBC) can be used in conjunction with receiver and transmitter diversity in order to increase the communication system's performance. For these systems, channel estimation and tracking must be performed since the receiver requires channel state information for decoding. In this thesis, block-type and comb-type channel estimation algorithms for OFDM systems over multipath fading channels are studied and simulated. Performance results using simulated frequency-selective channels are presented.

THIS PAGE INTENTIONALLY LEFT BLANK

TABLE OF CONTENTS

LIST OF FIGURES

LIST OF TABLES

THIS PAGE INTENTIONALLY LEFT BLANK

LIST OF ACRONYMS AND ABBREVIATIONS

AWGN	Additive White Gaussian Noise
A/D	Analog to Digital
BER	Bit Error Rate
D/A	Digital to Analog
dB	decibel
DFT	Discrete Fourier Transform
FFT	Fast Fourier Transform
HT	Hilly Terrain
ICI	Inter Carrier Interference
IDFT	Inverse Discrete Fourier Transform
IFFT	Inverse Fast Fourier Transform
ISI	Inter Symbol Interference
LOS	Line of Sight
LS	Least Square
LTV	Linear Time-varying
MIMO	Multiple Input Multiple Output
MISO	Multiple Input Single Output
MRC	Maximal Ratio Combining
MSE	Mean Square Error
NLOS	Non-Line of Sight
OFDM	Orthogonal Frequency Division Multiplexing
PSK	Phase Shift Keying
QAM	Quadrature Amplitude Modulation
SIMO	Single Input Multiple Output
SISO	Single Input Single Output
STBC	Space Time Block Coding
STC	Significant Tap Catching
SNR	Signal to Noise Ratio
TDL	Tapped Delay Line
TU	Typical Urban Area
WSSUS	Wide Sense Stationary Uncorrelated Scattering

THIS PAGE INTENTIONALLY LEFT BLANK

ACKNOWLEDGMENTS

First of all, I want to thank to my thesis advisors Prof. Roberto CRISTI and Prof. Murali TUMMALA for the valuable guidance and support they provided. I'm very proud that I had the chance to work with them.

Surely, my family gave me the greatest support during my studies at NPS as they have always done. Thank you Zeki SEN and Nebahat SEN for being so nice to me and thank you grandmother, Hanife EROZDEMIR and grandfather, Hayrettin EROZDEMIR for being a part of my life.

I promise to do my best for my country and walk in the path of the Great Founder of Turkish Republic, Mustafa Kemal Atatürk.

THIS PAGE INTENTIONALLY LEFT BLANK

EXECUTIVE SUMMARY

High-data-rate wireless communication has become more and more important for military and commercial applications. Orthogonal frequency division multiplexing (OFDM) seems to be a promising solution for increasing a communication system's data rate by utilizing the available bandwidth in the most efficient way. Furthermore, the use of multiple receive and transmit antennas greatly increases the channel capacity and the performance over frequency-selective channels.

In order to operate in the most effective way, OFDM-based communication systems need accurate channel estimation. This can be a challenging problem when the channel itself is time-varying due to changing geometry and Doppler frequency shift.

The objective of this thesis was to investigate the performances of various channel estimation techniques for OFDM systems with one or more transmit antennas. For a transmitter diversity OFDM system, we cannot use the same channel estimation techniques utilized for a single-transmit antenna system, due to the interference at the receiver caused by the multiple transmit antennas. In this research, we addressed the channel estimation problem of single-input multiple-output (SIMO) and multiple-input multiple-output (MIMO) systems. For SIMO and MIMO systems, the use of maximal ratio combining (MRC) and space-time block coding (STBC) would improve the performance in terms of channel capacity.

For the SIMO case, Matlab simulations of the OFDM systems utilizing least-square (LS), modified LS and comb-type channel estimation techniques have been performed. On the other hand, for the MIMO case, basic, simplified, significant tap catching (STC) and comb-type channel estimation techniques have been simulated. In all cases, discrete mobile multipath fading and additive white Gaussian noise (AWGN) channels have been chosen as simulated channels. The bit error rate (BER) performances of the simulated communication systems were obtained. A performance comparison between the OFDM systems utilizing different channel estimation methods was conducted.

For the SIMO systems, it was observed that the modified LS channel estimator performed better than the LS channel estimator for a wide range of signal-to-noise ratios (SNR). All channel estimators' performances degraded as the Doppler shift of the channel increased. However, the degradation was negligible for the comb-type channel estimator due to the insertion of the pilots in each of the transmitted OFDM blocks.

For the MIMO systems, the simulations showed that using a simplified channel estimation method utilizing STC does not degrade performance significantly at low values of the SNR. It was observed that the STC method performed better as the number of taps used was increased. Both the block-type and the comb-type channel estimators' performances degraded as the Doppler frequency increased. The reason why the comb-type channel estimator's performance degraded this time was that we did not insert pilots in every OFDM block as we have done for the SIMO case.

I. INTRODUCTION

Orthogonal frequency division multiplexing (OFDM) has emerged as an attractive technique for achieving high-bit-rate data transmission with high bandwidth efficiency in frequency-selective multipath fading channels.

In order to make OFDM more reliable, several transmitter and receiver diversity techniques utilizing space-time or space-frequency codes can be used. Space-time block coding (STBC) is based on Alamouti transmitter diversity scheme [1] and one of the most efficient coding techniques that can be applied with transmitter diversity systems [2].

A key issue with coherent OFDM systems is the need for channel state information. This could be avoided by using differential phase-shift keying (DPSK) at the expense of a loss of 3-4 dB in signal-to-noise ratio (SNR) [3].

Channel estimation methods are generally divided into two groups: block-type and comb-type. In a block-type channel estimation method, all the sub-carriers in an OFDM block are used as pilot tones, and the OFDM block is transmitted periodically. In a comb-type channel estimation method, some of the sub-carriers are used as pilot tones in each of the OFDM blocks transmitted. In the block-type case, since all the sub-carriers are used to transmit pilot tones, it is possible to obtain an accurate estimate of the channel coefficients. In subsequent blocks, we can track variations of the channel coefficients by generating reference symbols. This increases the computational complexity of the channel estimator. In a comb-type channel estimation algorithm, an interpolation method must be used in order to estimate the frequency response of the channel at all sub-carrier frequencies. As a result of the interpolation operation, some error occurs. The interpolation error can be reduced by increasing the number of pilot sub-carriers, but this also decreases the bandwidth efficiency. In conclusion, both channel estimation techniques have their own advantages and disadvantages.

A. OBJECTIVE

For OFDM systems utilizing coherent demodulation, perfect channel estimation is critical in terms of low BER performance. Unlike for systems with a single-transmit antenna, the channel estimation process for OFDM systems with multiple transmit

antennas is complex. The main objective of this thesis was to investigate the performances of various block-type and comb-type channel estimators over OFDM systems with and without transmitter diversity in multipath fading channels.

In this thesis, the first step was to introduce the fundamentals of OFDM and its combination with maximal ratio combining (MRC) [4] and STBC. Subsequently, we studied various published techniques of channel estimation for OFDM systems with a single-transmit antenna and with transmitter diversity. As the last step, several OFDM communication systems with and without transmitter diversity employing various channel estimation techniques were developed in Matlab, and simulation results are presented in graphical form.

In order to observe the channel estimation performances over OFDM systems, we built discrete multipath channels with different profiles.

B. RELATED RESEARCH

Transmitter and receiver diversity have been used with OFDM systems in order to improve their performance. Several low complexity block-type and comb-type channel estimation techniques for single-transmit antenna systems, some of which use channel's time-domain properties, have been proposed in [3, 5, 6]. For transmitter diversity systems utilizing STBC, we cannot use the same channel estimation algorithms we use for single-transmit antenna systems. This stems from the fact that each received signal is the superposition of all transmitted signals, thus making it difficult to separate various channels. Several channel estimation algorithms, both block-type and comb-type, which address this interference problem have been proposed in [7, 8, 9].

While performing Matlab simulations, the channel model we use also plays an important role. Mobile wireless multipath fading channels can be simulated by discrete multipath channel models [10] with desired properties.

C. ORGANIZATION OF THE THESIS

This thesis is organized into six chapters and two appendices. Chapter II introduces the characterization of mobile wireless multipath fading channels and presents a simulation model for discrete multipath channels. Chapter III introduces basic principles of OFDM and gives the input-output relations of systems utilizing MRC or

STBC. Chapter IV discusses several channel estimation techniques for single and multiple-transmit antenna systems. Chapter V presents the Matlab simulation results of the communication systems utilizing the proposed channel estimation techniques. Chapter VI provides a summary of the thesis, conclusions and suggestions for future studies.

Appendix A lists the parameters of the multipath channels used in this thesis. Appendix B provides explanations for the Matlab code.

THIS PAGE INTENTIONALLY LEFT BLANK

II. MOBILE WIRELESS MULTIPATH FADING CHANNELS

Multipath and fading are two important issues in radio communication systems which have to be well understood in order to design a reliable and efficient communication system.

Multiple paths occur due to the fact that there is always atmospheric scattering and refraction, or there are reflections from objects in the propagation environment. Multiple paths affect the signal arriving at the receiving antenna both destructively and constructively, causing different attenuations and delays to the transmitted signal [10].

Multipath fading affects the signal's spectrum in both time and frequency. In a frequency-selective channel, multiple arrivals of the transmitted signal to the receiver with different time delays, phases and amplitudes cause the frequency response of the channel not to be flat over the bandwidth of the signal. In addition, the motion of the transmitter or the receiver results in changes in multipath due to terrain effects and buildings in the propagation environment. The atmospheric changes also result in changes in multipath even if the transmitter and the receiver are fixed.

In this chapter, we discuss lowpass-equivalent and statistical characterization of discrete multipath fading channel models and build a time-varying discrete multipath channel for simulation purposes.

A. CHARACTERIZATION OF A DISCRETE MULTIPATH CHANNEL MODEL

When there are obstacles and reflectors in the radio propagation channel, the transmitted signal arrives at the receiver following different paths. These paths altogether constitute the multipath fading channel.

Multipath is usually described by line-of-sight (LOS) and non-line-of-sight (NLOS) components. A LOS path has a direct connection between the transmit antenna and the receive antenna. All other paths the signal follows after being reflected from various obstacles are NLOS paths. Illustration of a multipath environment is shown in Figure 1.

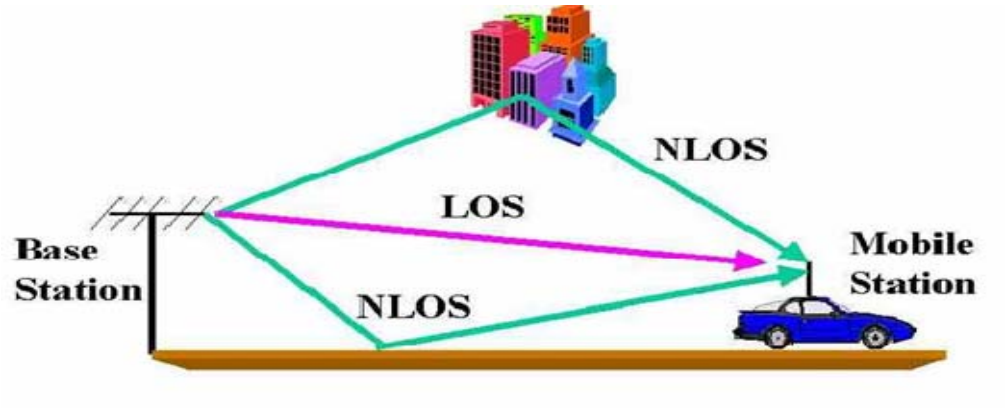

Figure 1. Illustration of multipath environment (From Ref. [11].)

1. Lowpass-Equivalent Characterization of Discrete Multipath Channels

A discrete multipath channel model defines the channel with a finite number of multipath components reflected by small hills, buildings and other obstacles in open areas and rural environments. We define the discrete multipath channel as a linear time-varying (LTV) system as shown in Figure 2.

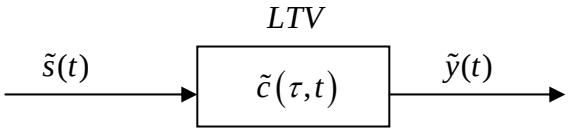

Figure 2. Linear time-variant (LTV) channel

The output signal of the LTV system can be expressed as

$$\tilde{y}(t) = \sum_n \tilde{a}_n(\tau_n, t)\,\tilde{s}\left(t - \tau_n(t)\right) \tag{2.1}$$

where $\tilde{y}(t)$ is the complex envelope of the output signal, $\tilde{a}_n(t)$ is the attenuation factor of the n^{th} multipath, $\tilde{s}(t)$ is the baseband input signal, and $\tau_n(t)$ is the propagation delay of the n^{th} multipath component. The *lowpass-equivalent channel impulse response* $\tilde{c}(\tau,t)$ can then be expressed as [10]

$$\tilde{c}(\tau,t) = \sum_n \tilde{a}_n\left(\tau_n(t),t\right)\delta\left(\tau - \tau_n(t)\right) \tag{2.2}$$

As seen from the above equation, the time-varying channel has two time variables. The variable t shows the time the observation is made at the channel output when an impulse is applied at time $(t-\tau)$. By taking the Fourier transform of the impulse

response with respect to the variable τ , we can define the *channel frequency response* as

$$\tilde{C}(f,t) = \int_{-\infty}^{\infty} \tilde{c}(\tau,t) e^{-j2\pi f\tau} d\tau \tag{2.3}$$

As the channel changes with respect to the variable *t*, both the time and the frequency-domain representations of the channel are affected.

Due to the mobility of the transmitter or the receiver, or the motion of the surrounding objects in the propagation environment, the wireless channel is linear but time-varying. This time-varying behavior is characterized by *Doppler shifts* in the frequency-domain, which result in frequency broadening of the frequency spectrum of the transmitted signal. The *Doppler frequency* shift caused by relative motion between transmitter and receiver is given by

$$f_d = \frac{s}{\lambda} \tag{2.4}$$

where *s* is the relative velocity between transmitter and receiver and λ is the transmitted signal's wavelength. A more general definition in terms of channel characteristics is the *Doppler spread function* that can be found by taking the Fourier transform of the channel frequency response with respect to the variable *t*:

$$H(f,v) = \int_{-\infty}^{\infty} \tilde{C}(f,t) e^{-j2\pi vt} dt \tag{2.5}$$

The last channel function we will define is the *delay-Doppler spread function* which is given as the Fourier transform of the channel impulse response with respect to *t*:

$$H(\tau,v) = \int_{-\infty}^{\infty} \tilde{c}(\tau,t) e^{-j2\pi vt} dt \tag{2.6}$$

All the lowpass-equivalent channel functions defined so far characterize the channel in time and frequency. We can describe the relation between all channel functions as shown in Figure 3.

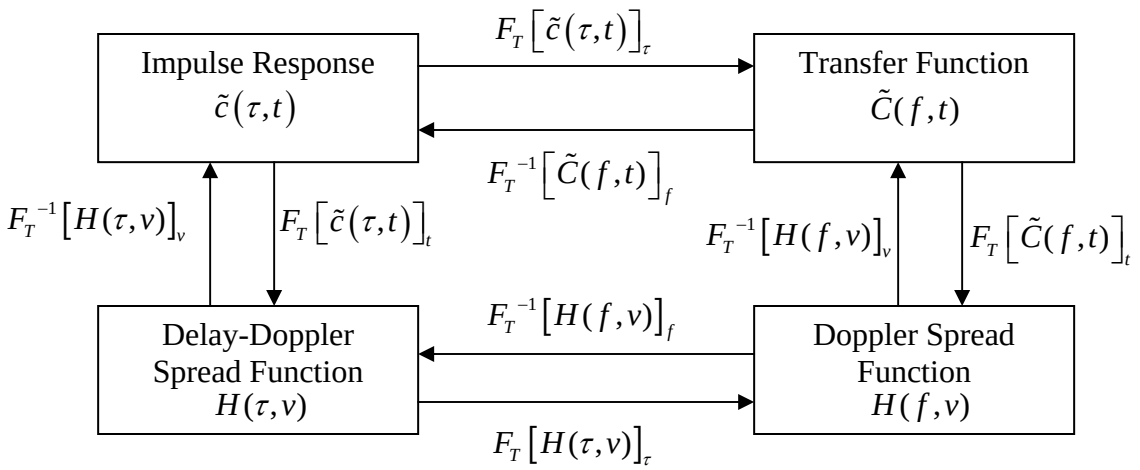

Figure 3. Relation between channel functions

2. Wide Sense Stationary Uncorrelated Scattering (WSSUS) Model and Power Spectrum Functions of Discrete Multipath Channels

A lowpass-equivalent channel impulse response, $\tilde{c}(\tau,t)$, can be modeled as a complex Gaussian process in *t* by using the central limit theorem since the components of the multipath signal are results of the reflections and scatterings from the various obstacles in the environment. The time-varying nature of the channel is modeled as a wide sense stationary (WSS) random process in *t* with the *autocorrelation function*

$$R_{\tilde{c}}(\tau_1,\tau_2,\Delta t) = E\left[\tilde{c}^*(\tau_1,t)\tilde{c}(\tau_2,t+\Delta t)\right] \tag{2.7}$$

where the superscript $(.)^*$ denotes complex conjugate. By using the uncorrelated scattering (US) assumption, as the attenuation and the delay of distinct paths are independent of each other in the multipath channel, the autocorrelation function can be rewritten as

$$R_{\tilde{c}}(\tau_1,\tau_2,\Delta t) = R_{\tilde{c}}(\tau_1,\Delta t)\delta(\tau_1-\tau_2) \tag{2.8}$$

As a consequence, we make the following assumptions:

1. $\tilde{c}(\tau,t)$ is a WSS process with zero mean,

2. $\tilde{c}(\tau_1,t), \tilde{c}(\tau_2,t)$ are uncorrelated if $\tau_1 \neq \tau_2$

Then, we can define

$$R_{\tilde{c}}(\tau,\Delta t) = E\left[\tilde{c}^*(\tau,\Delta t)\tilde{c}(\tau,t+\Delta t)\right] \tag{2.9}$$

The above equation is called the WSSUS model for a fading channel [10].

By taking the Fourier transform of the autocorrelation function of the channel with respect to Δt, we can find the *scattering function of the channel* as

$$S(\tau, v) = F_T\left[R_{\tilde{c}}(\tau, \Delta t)\right]_{\Delta t} = \int_{-\infty}^{\infty} R_{\tilde{c}}(\tau, \Delta t) e^{-j2\pi v \Delta t} d\Delta t \tag{2.10}$$

The scattering function shows how fast the channel changes with respect to the Doppler frequency *v* and the time delay *τ*. By using the scattering function, we can obtain some other important statistical functions of the channel. The *Delay power spectral density*, also called the *delay power profile* or the *multipath intensity profile*, can be found by

$$p(\tau) = \int_{-\infty}^{\infty} S(\tau, v) dv \tag{2.11}$$

and it represents the average received power as a function of the propagation delay τ. The nominal width of the delay power profile is called the *maximum delay spread* T_m.

The *Doppler power spectrum* is another function that can be found by using the scattering function of the channel:

$$S(v) = \int_{-\infty}^{\infty} S(\tau, v) d\tau \tag{2.12}$$

The Doppler power spectrum shows the time variation characteristics of the channel. The range over which the Doppler power spectrum is essentially nonzero is called the Doppler Spread of the channel f_d.

It is clearly seen that taking the integral of the channel scattering function with respect to the time delay variable gives us the delay power profile while taking the integral of the scattering function with respect to the Doppler shift variable gives us the Doppler power spectrum.

B. SIMULATING A DISCRETE MULTIPATH CHANNEL MODEL

In order to simulate a discrete multipath channel efficiently, we used a uniformly spaced tapped-delay-line (TDL) model presented in this section.

1. Uniformly Spaced TDL Model

In order to describe a discrete multipath channel model, we need to generate time-varying delays and tap gains. The lowpass equivalent impulse response of the channel as given in (2.2) becomes

$$\tilde{c}(\tau,t) = \sum_{k=1}^{K(t)} \tilde{a}_k(\tau_k(t),t)\,\delta(\tau-\tau_k(t)) \tag{2.13}$$

As it is seen, the number of taps $K(t)$, the tap delays $\tau_k(t)$ and the tap gains $\tilde{a}_k(\tau_k(t),t)$ are considered to be variable with time. Under these considerations, the lowpass-equivalent output of the channel can also be written as

$$\tilde{y}(t) = \sum_{k=1}^{K(t)} \tilde{a}_k(\tau_k(t),t)\,\tilde{s}(t-\tau_k(t)) \tag{2.14}$$

where $\tilde{s}(t)$ is the input lowpass signal. In most reference channel models, using the assumption that the number of discrete components is almost constant and the delays change very slowly, the variable tap gains, delays and number of taps are considered to be constant [10]. Under these circumstances, the lowpass equivalent channel impulse response and the lowpass-equivalent output of the channel can be rewritten as

$$\tilde{c}(\tau,t) = \sum_{k=1}^{K} \tilde{a}_k(t)\,\delta(\tau-\tau_k) \tag{2.15}$$

$$\tilde{y}(t) = \sum_{k=1}^{K} \tilde{a}_k(t)\,\tilde{s}(t-\tau_k) \tag{2.16}$$

In order to make the simulation realistic, we need to account for shaping filters at the transmitter and receiver. These are raised-cosine lowpass filters with bandwidth *B*, the bandwidth of the transmitted signal. Figure 4 shows the block diagram of the process relating the transmitted and received signals.

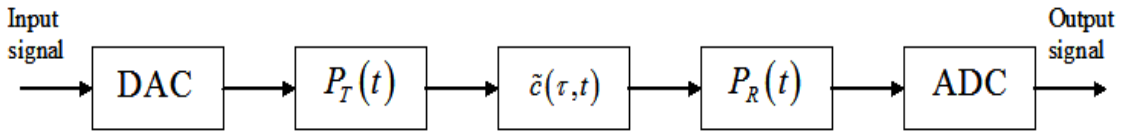

Figure 4. The channel impulse response and the shaping filters

In the ideal case, we can approximate the combined effect of the shaping filters by

$$P_T(t) * P_R(t) = \mathrm{sinc}(Bt) \tag{2.17}$$

where $*$ denotes the convolution operation. In this case, the overall channel has impulse response

$$\tilde{c}(\tau,t) = \sum_{k=1}^{K} \tilde{a}_k(t)\,\mathrm{sinc}(B(\tau_k-\tau)) \tag{2.18}$$

The output of the channel $\tilde{y}(t)$ in Equation (2.16) can be obtained by using a TDL channel model to which $\tilde{s}(t)$ is the input. In this channel model, the time delay values of the paths are arbitrary, and not integer multiples of the sampling time. In this way, the combined impulse response of the channel and the shaping filters can be computed using a uniformly spaced TDL with impulse response [10]

$$\tilde{g}_n(t) = \sum_{k=1}^{K} \tilde{a}_k(t)\,\mathrm{sinc}\big(B(\tau_k - nT)\big) = \sum_{k=1}^{K} \tilde{a}_k(t)\,\gamma(k,n), \quad 0 \le n \le N \tag{2.19}$$

$$\gamma(k,n) = \mathrm{sinc}\left[\frac{\tau_k}{T} - n\right] \tag{2.20}$$

where $T = B^{-1}$ is the symbol duration. According to the delay profile of the channel, the energy $\tilde{a}_k(t)$ from the k^{th} path is spread to all time delays by the term $\gamma(k,n)$. The number of taps can be chosen according to the maximum delay spread T_m of the channel. The discrete time representation of a uniformly spaced TDL model with *N+1* taps is shown in Figure 5.

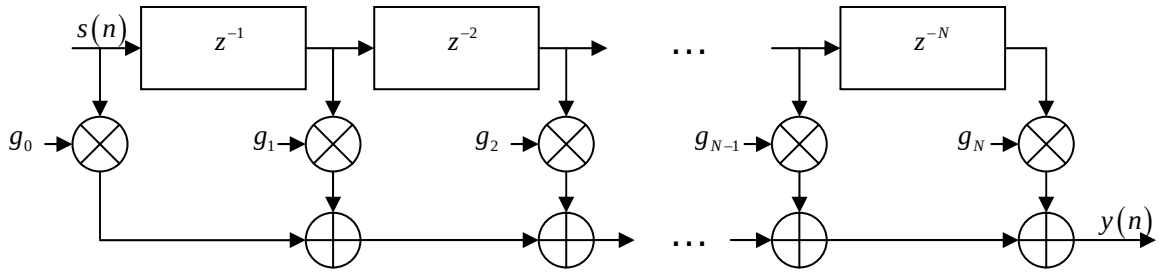

Figure 5. The discrete time representation of a uniformly spaced TDL model

2. Generation of Tap-Gain Processes

Generation of tap-gain processes is the other important issue in modeling a discrete multipath channel. We start with generating *K* independent and zero mean discrete time Gaussian processes by using random number generators where *K* represents the number of paths in the power delay profile we use. After generating the Gaussian processes, the shape of the desired power spectral density must be applied to these processes to make them have the common Doppler spectrum $S(f)$. We use the Jakes spectrum which is a commonly used Doppler spectrum in channel modeling and it is given by [12]

$$S(f) = \frac{A}{\left[1 - \left(\frac{f}{f_d}\right)^2\right]^{1/2}}, \; f \in [-f_d, f_d] \tag{2.21}$$

where f_d is the maximum Doppler frequency. The shape of the Jakes spectrum is applied to the independent processes by using appropriate shaping filters. The shaping filter is considered to have a frequency response $H(f) = \sqrt{S(f)}$ which is real and symmetric [10]. After applying the shaping filters, the processes should be normalized as having unit power. In order to make the discrete channel components have the average powers specified by the delay power profile of the channel, we should scale them with the corresponding path gain factors which are denoted as σ_k for $k = 1, 2, ..., K$.

A generic block diagram showing the generation of bandlimited tap-gain processes is presented in Figure 6.

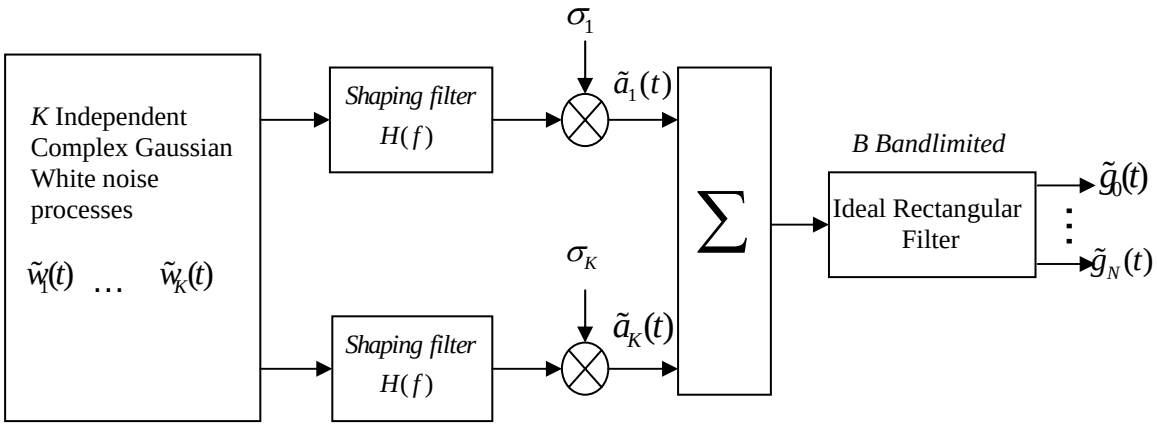

Figure 6. Generation of bandlimited tap-gain processes

In cases where the bandwidth of the input signal is much larger than the bandwidth of the tap-gain filter which is equal to f_d, the tap-gains are generated at a lower sampling rate and interpolated to the desired rate.

3. Reference Channel Models

In our simulations, we used the reduced profiles for *Typical Urban Area (TU)* and *Hilly Terrain (HT)* environments which are given in [10]. These are 6-path channel models each with the Jakes spectrum with an added Ricean $K-$ *factor* , which shows the

power ratio between LOS and NLOS components. Figures 7 and 8 show the multipath intensity profiles of these reference models. Detailed parameter information of these channels can be found in Appendix A.

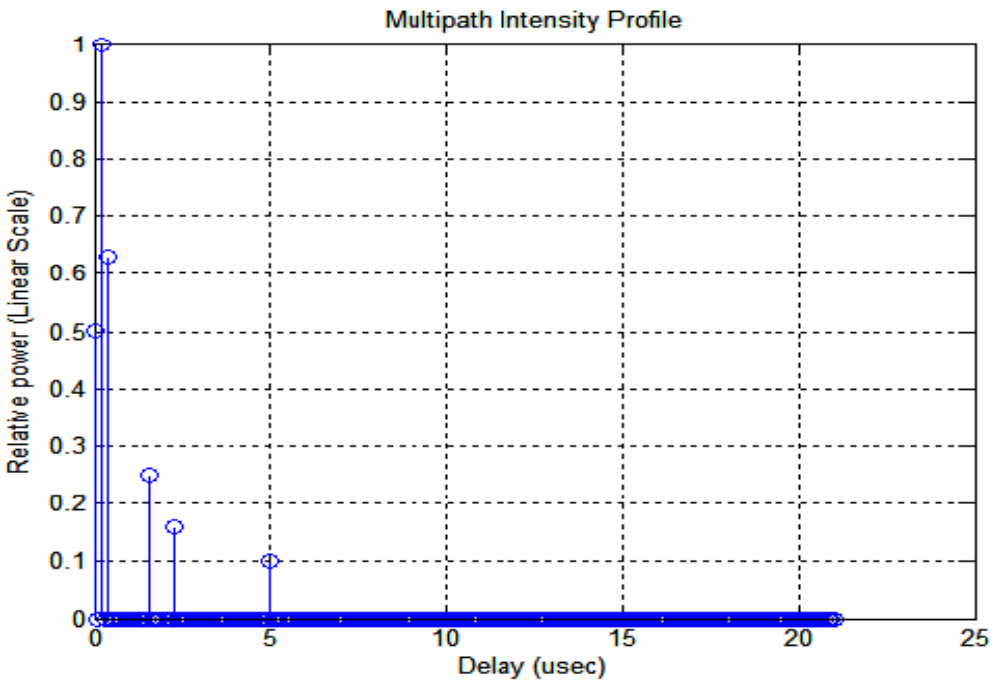

Figure 7. TU multipath intensity profile

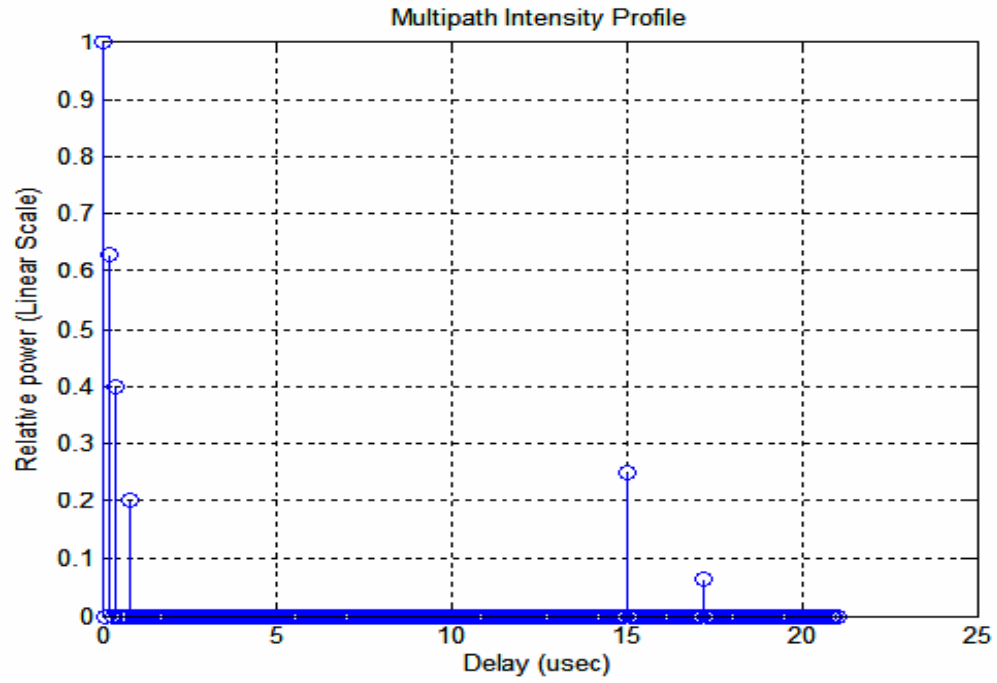

Figure 8. HT multipath intensity profile

C. SUMMARY

In this chapter, we gave a brief explanation of lowpass-equivalent and statistical characterization of discrete multipath channel models. We presented a general concept of designing a uniformly spaced TDL channel model and showed the generation of tap-gain processes. The reference channel models which we used in our simulations are also discussed.

In the next chapter, we will present an Alamouti-scheme based STBC technique [1] and its combination with OFDM.

III. SPACE-TIME BLOCK CODING-ORTHOGONAL FREQUENCY DIVISION MULTIPLEXING (STBC-OFDM) SYSTEMS

The demand for high-speed and reliable data transmission increases everyday. Changing nature of today's world also increases the need for efficient communication systems for mobile users. OFDM has proven to be a solution due to its simplicity and effectiveness in frequency-selective environments and it has been adopted by several wireless standards such as the IEEE 802.11a local area network (LAN) and the IEEE 802.16a metropolitan area network (MAN). OFDM compensates the effects of frequency-selective fading by dividing the entire bandwidth of a wideband channel into flat-fading narrowband sub-channels [3].

In order to reduce the BER, OFDM may be combined with error correction coding techniques and various diversity methods. Alamouti-based space-time coding technique is one of the most effective transmitter diversity methods and when combined with OFDM, it enhances the system performance [13].

In this chapter, we present the general structure of a system employing OFDM and its combination with STBC techniques.

A. OFDM SYSTEMS

OFDM is a very effective multicarrier technique, which produces solutions for a number of important issues in wireless communications. It allows the most efficient use of the available bandwidth, prevents inter carrier interference (ICI), and reduces the effect of frequency-selective fading on transmitted signals, which is seen as inter symbol interference (ISI).

In OFDM, a high-data-rate stream is divided up into K parallel data streams of lower data-rate sub-carriers, which are transmitted simultaneously. OFDM sub-carriers are designed such that they are orthogonal to each other. This allows them to be used in a spectrally overlapped manner, which enables the maximum use of the available bandwidth.

The choice of orthogonal sub-carriers allows the spectrum of each sub-carrier to

have a null at the other sub-carrier frequencies so that ICI is avoided. Modulation by an orthogonal sub-carrier is easily implemented by the inverse fast Fourier transform (IFFT) operation.

By turning a high-data-rate stream into parallel lower data rate streams, the symbol period is increased and frequency-selective fading becomes flat fading. In this way, the ISI caused by a frequency-selective fading channel is mitigated by OFDM. Multipath spread of the channel also causes ISI and this can be mitigated by adding a guard interval to the transmitted signal.

The block diagram of an OFDM-based communication system is shown in Figure 9. Each of the blocks will be explained in the following discussion.

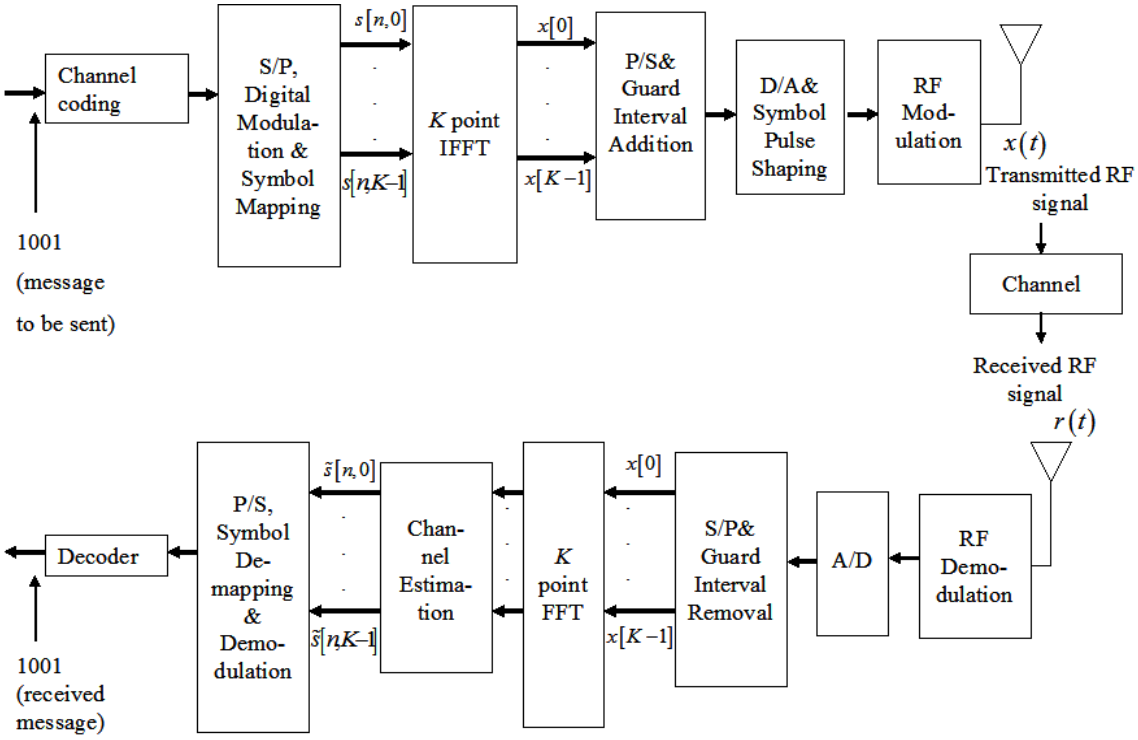

Figure 9. Block diagram of an OFDM system (After Ref. [13])

1. Channel Coding

In order to increase the performance of the OFDM system, channel coding is applied to the sequential binary input data. In this thesis, we used the IEEE 802.11a standard's convolutional encoder for forward error correction (FEC). In most applications, interleaving is also used along with FEC to correct burst errors. Since our

main focus in this thesis was to study channel estimation techniques, we did not use any interleaver.

The convolutional encoder we consider has a rate of 1/2, constraint length 7 and generator polynomials (171,133) in octal form as defined in the IEEE 802.11a standard [14].

2. Digital Modulation and Symbol Mapping

According to the modulation technique used, symbol mapping is performed. After the symbol mapping, we have a complex envelope of the digitally modulated data.

3. IFFT

After the symbol mapping process, a *K*-point IFFT is applied to the complex data symbols where *K* represents the number of orthogonal sub-carrier frequencies used.

We can represent the complex baseband equivalent signal by

$$\tilde{s}(t) = \frac{1}{K}\sum_{k=0}^{K-1} \tilde{A}_k(t) e^{j2\pi k\Delta f t} \tag{3.1}$$

where Δf is the frequency separation between each sub-carrier pair and $\tilde{A}_k(t)$ is the complex amplitude for the k^{th} sub-carrier. The term $\frac{1}{K}$ in Equation (3.1) is inserted for convenience. Supposing that the total symbol period is T_s seconds by sampling $\tilde{s}(t)$ every $\frac{T_s}{K}$ seconds, we obtain a block of *K* data points defined as

$$x_n = \tilde{s}(nT_s/K) = \frac{1}{K}\sum_{k=0}^{K-1} \tilde{A}_k e^{j2\pi kn\Delta f T_s/K},\ n = 0,1,...,K-1 \tag{3.2}$$

Choosing $\Delta f T_s = 1$ for orthogonality yields

$$x_n = \frac{1}{K}\sum_{k=0}^{K-1} \tilde{A}_k e^{j2\pi kn/K},\ n = 0,1,2,...,K-1 \tag{3.3}$$

Equation (3.3) is equivalent to the inverse discrete Fourier transform (IDFT) operation [15], and it shows modulation of the data $\tilde{A}_k$ by the sub-carriers with digital frequencies $\frac{k2\pi}{K}$.

In our simulations, we used a 128-point fast Fourier transform (FFT). The length of the IFFT output is called the OFDM symbol time, denoted as T_s.

4. Guard Interval Addition

In order to prevent the ISI caused by multipath delay spread, a *guard interval* is added to the OFDM symbol time T_s. The important point is that the guard interval should be larger than the expected delay spread of the channel in order to eliminate ISI caused by the adjacent OFDM symbols.

The guard interval is denoted as T_g and specified as a fraction of T_s. In our simulations, we used a cyclic prefix extension obtained from the last $m = \frac{T_s}{T_g}$ samples of the IFFT output and added it to the beginning of the OFDM tones. By using a cyclic prefix extension, the linear convolution between the transmitted signal and the channel impulse response becomes a circular convolution. In this way, we prevent both ISI and ICI since orthogonality between sub-carriers is maintained.

The total time interval including the cyclic prefix is called the OFDM *block time* and it is denoted as T_b. Optional cyclic prefix ratios used in our simulations are 1/4, 1/8, 1/16 and 1/32. It should be noted that as the length of the cyclic prefix increases, the effective throughput decreases. As a consequence, the cyclic prefix length should be chosen so that the data rate is minimally affected.

5. Digital to Analog (D/A) Conversion and Symbol Pulse Shaping

After the cyclic prefix addition, D/A conversion is performed and the signal becomes a continuous time baseband signal.

Since each OFDM symbol has a finite time duration, spectral leakage causes interchannel interference. One way to solve this problem is by setting some of the sub-carrier frequencies at the edges as nulls. Another way of solving this problem is by shaping the OFDM symbol's spectrum either by a time-domain window or by filtering.

6. RF Modulation-Demodulation

The last step in the transmitter side is RF modulation of the signal. The OFDM symbols are upconverted to a specified radio frequency carrier, amplified and transmitted through the antenna.

At the receiver, the signal is downconverted to baseband, sampled by an analog to digital (A/D) converter and passed to the FFT processor.

In this thesis, all the simulations are conducted at the baseband level.

7. Guard Interval Removal and FFT operation

The guard interval is removed from the received OFDM block, and only the information bearing part of the OFDM block is demodulated by the FFT into the individual sub-carrier components. These frequency-domain data samples are then used to get the channel state information and the estimate of the original transmitted symbol.

8. Channel Estimation

To be able to estimate the original transmitted OFDM symbol, we need accurate channel state information [4]. Channel state information can be obtained by using transmitted data and pilot tones.

There are various channel estimation techniques, and the ones examined in this thesis will be explained in detail in Chapter IV.

9. Symbol Demapping and Decoding

After getting the channel state information and estimating the original transmitted OFDM symbol, demapping is performed according to the constellation used at the transmitter. As the last step, demapped symbols are processed through a Viterbi decoder.

B. ALAMOUTI-BASED STBC TECHNIQUE COMBINED WITH OFDM

By using multiple transmit and/or receive antennas, the communication system performance can be enhanced. In [1], the Alamouti transmitter diversity scheme has been proposed, and it has been shown that using two transmit antennas and one receive antenna provided the same diversity performance as a MRC scheme with one transmit antenna and two receive antennas without any requirement for bandwidth expansion.

The Alamouti transmitter diversity scheme was proposed for flat fading channels. In [2], the Alamouti-scheme is further extended to frequency-selective fading channels

under the name of STBC, which enhances the system performance by exploiting diversity in both space and time-domains. When STBC and OFDM are combined, a high-data-rate communication system can be implemented.

In our simulations, we investigated various channel estimation performances over systems with receiver and/or transmitter diversity. There is no difference between a single-input single-output (SISO) and a single-input multiple-output (SIMO) system in terms of the channel estimation techniques explained in this thesis. The channel estimation algorithms for multiple-input single-output (MISO) and multiple-input multiple-output (MIMO) systems are also the same. This subject will be explained in Chapter IV in more detail. In what follows, we introduce SIMO and MIMO diversity schemes.

1. Single-Input Multiple-Output (SIMO)-OFDM Systems

A SIMO-OFDM system utilizing a MRC scheme is shown in Figure 10, and it consists of one transmit antenna and two receive antennas.

The channels are represented as continuous-time filters with time-varying tap gains as introduced in Chapter II. The received signals at the antennas can be written as

$$\begin{aligned} r_1(t) &= h_1(t) * x(t) + w_1(t) \\ r_2(t) &= h_2(t) * x(t) + w_2(t) \end{aligned} \tag{3.4}$$

where $w_1(t)$ and $w_2(t)$ are noise components. The received signals contain information bearing data and added cyclic prefix.

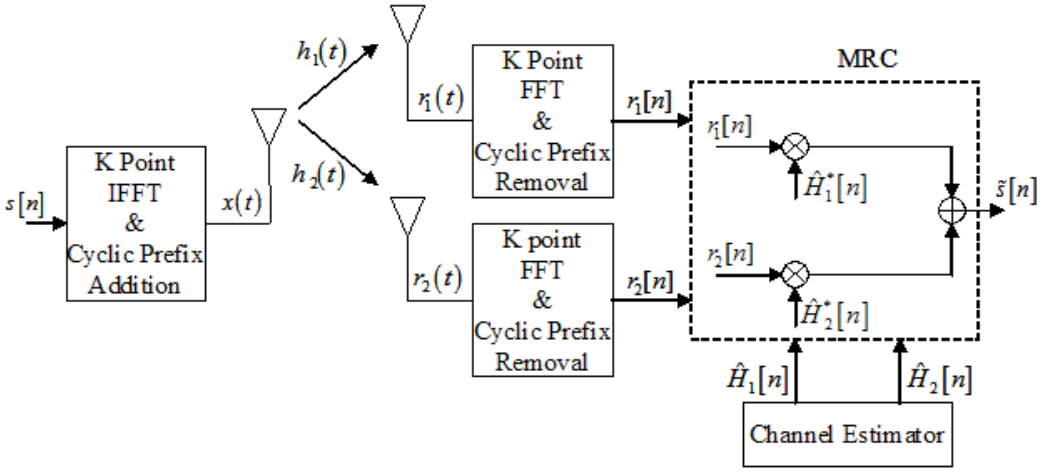

Figure 10. 1×2 SIMO-OFDM system utilizing MRC

The cyclic prefix is removed and the *K* point FFT of the information bearing data is taken. The output of the FFT for the i^{th} antenna at the n^{th} OFDM block and k^{th} tone can be written as

$$r_i[n,k] = H_i[n,k]s[n,k] + w_i[n,k] \tag{3.5}$$

where $w_i[n,k]$ is additive Gaussian with zero mean and variance ρ. We assume that $w_i[n,k]$ is independent for different *n*'s, *k*'s and *i*'s. The frequency response of the channel corresponding to the i^{th} receive antenna at the n^{th} OFDM block and k^{th} tone is denoted as $H_i[n,k]$. The FFT output is sent to the MRC and the estimate of the transmitted OFDM symbol is computed using channel state information by [1]

$$\tilde{s}[n,k] = \hat{H}_1^*[n,k]r_1[n,k] + \hat{H}_2^*[n,k]r_2[n,k] \tag{3.6}$$

where $\hat{H}_1[n,k]$ and $\hat{H}_2[n,k]$ are the estimated channel frequency responses. Substituting (3.5) into (3.6) we can rewrite the decoder equation as

$$\tilde{s}[n,k] = \left(\left|\hat{H}_1[n,k]\right|^2 + \left|\hat{H}_2[n,k]\right|^2\right)s[n,k] + \hat{H}_1^*[n,k]w_1[n,k] + \hat{H}_2^*[n,k]w_2[n,k] \tag{3.7}$$

By multiplying the complex conjugates of the estimated channel frequency responses with the corresponding received symbols, the MRC scheme compensates the phase shifts introduced by the channels. In this way, we obtain an estimate of the transmitted symbol which mostly depends on the magnitudes of the channel frequency responses rather than the phase components of the channels as given in Equation (3.7).

2. Multiple-Input Multiple-Output (MIMO)-OFDM Systems

A MIMO-OFDM system utilizing STBC with two transmit antennas and two receive antennas is shown in Figure 11.

In Figure 11, $b[n]$ is the digitally modulated signal at time *n*. STBC operation is performed over $b[n]$ and it is turned into two parallel information streams. The sequence of the transmitted data blocks can be represented as shown in Table 1.

OFDM block	Transmit Antenna-1	Transmit Antenna-2
n	$s_1[n]$	$s_2[n]$
n+1	$s_1[n+1]=-s_2^*[n]$	$s_2[n+1]=s_1^*[n]$

Table 1. Transmission sequence for STBC (After Ref. [1])

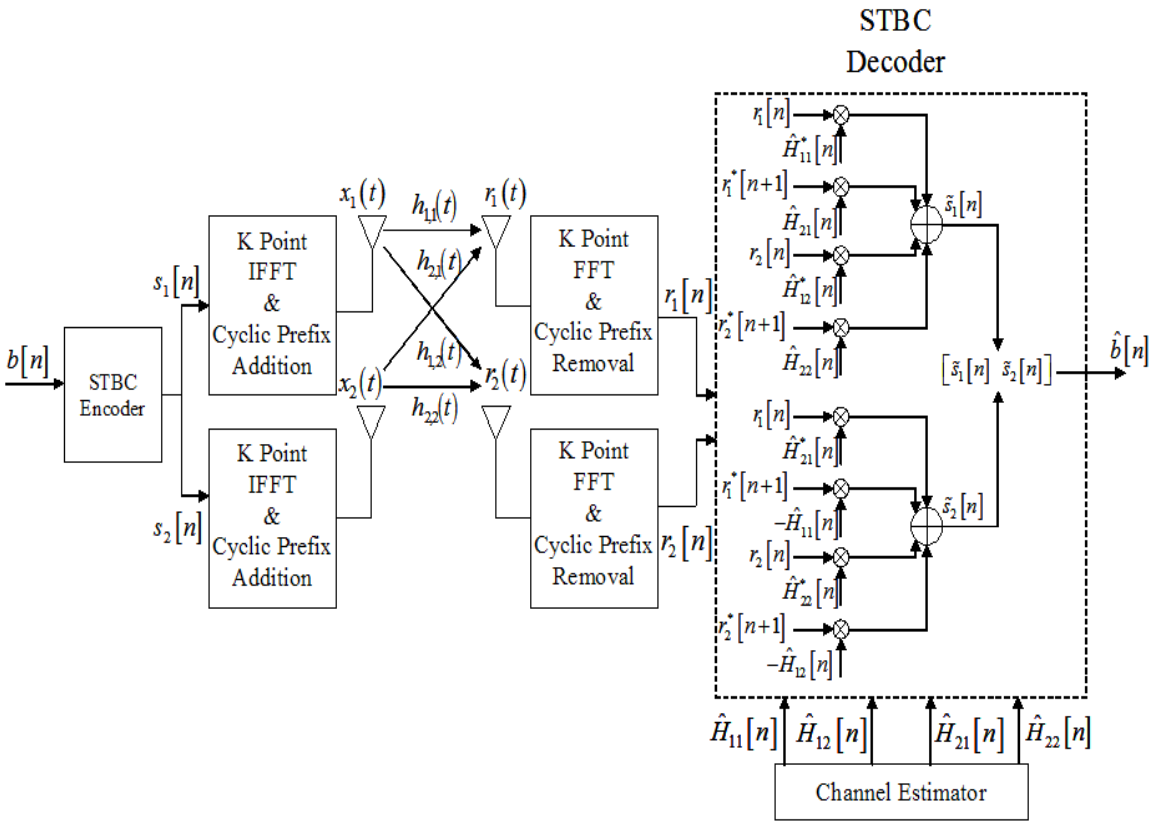

Figure 11. 2×2 STBC MIMO-OFDM system

By examining Table 1, we can see that the four encoded symbol blocks out of $b[n]$ are

$$
\begin{aligned}
s_1[n] &= [b[n,1], b[n,2], ..., b[n,K]] \\
s_2[n] &= [b[n,K+1], b[n,K+2], ..., b[n,2K]] \\
s_1[n+1] &= [-b^*[n,K+1], -b^*[n,K+2], ..., -b^*[n,2K]] \\
s_2[n+1] &= [b^*[n,1], b^*[n,2], ..., b^*[n,K]]
\end{aligned}
\tag{3.8}
$$

Assuming that the channels are quasi-static over two OFDM blocks, the received signals at the antennas are expressed by

$$\begin{aligned} r_1(t) &= h_{11}(t) * x_1(t) + h_{21}(t) * x_2(t) + w_1(t) \\ r_2(t) &= h_{12}(t) * x_1(t) + h_{22}(t) * x_2(t) + w_2(t) \\ r_1(t+T_s) &= h_{11}(t) * x_1(t+T_s) + h_{21}(t) * x_2(t+T_s) + w_1(t+T_s) \\ r_2(t+T_s) &= h_{12}(t) * x_1(t+T_s) + h_{22}(t) * x_2(t+T_s) + w_2(t+T_s) \end{aligned} \tag{3.9}$$

where $h_{ij}(t),\ i=1,2\ j=1,2,$ are the continuous-time filter representations of the channels from i^{th} transmit antenna to the j^{th} receive antenna.

After the cyclic prefix removal and the FFT operation, the received signals at the k^{th} sub-carrier frequency are expressed by

$$\begin{aligned} r_j[n,k] &= \sum_{i=1}^{2} H_{ij}[n,k]\, s_i[n,k] + w_j[n,k] \\ r_j[n+1,k] &= \sum_{i=1}^{2} H_{ij}[n,k]\, s_i[n+1,k] + w_j[n+1,k] \end{aligned} \tag{3.10}$$

where the noise at each receiver has the same properties as it does in the SIMO case.

The outputs are sent to the STBC decoder and the estimates of the transmitted OFDM symbols are computed using channel state information provided by the channel estimator as [1, 2]

$$\begin{aligned} \tilde{s}_1[n,k] &= \hat{H}_{11}^*[n,k]\, r_1[n,k] + \hat{H}_{21}[n,k]\, r_1^*[n+1,k] + \hat{H}_{12}^*[n,k]\, r_2[n,k] + \hat{H}_{22}[n,k]\, r_2^*[n+1,k] \\ \tilde{s}_2[n,k] &= \hat{H}_{21}^*[n,k]\, r_1[n,k] - \hat{H}_{11}[n,k]\, r_1^*[n+1,k] + \hat{H}_{22}^*[n,k]\, r_2[n,k] - \hat{H}_{12}[n,k]\, r_2^*[n+1,k] \end{aligned} \tag{3.11}$$

where $\hat{H}_{ij}[n,k];\ i=1,2\ j=1,2,$ are the estimated frequency responses of the channels from the i^{th} transmit antenna to the j^{th} receive antenna.

By substituting (3.10) into (3.11) we obtain

$$\begin{aligned} \tilde{s}_1[n,k] &= \left(\left|\hat{H}_{11}[n,k]\right|^2 + \left|\hat{H}_{12}[n,k]\right|^2 + \left|\hat{H}_{21}[n,k]\right|^2 + \left|\hat{H}_{22}[n,k]\right|^2\right) s_1[n,k] + \hat{H}_{11}^*[n,k]\, w_1[n,k] + \\ &\quad \hat{H}_{21}[n,k]\, w_1^*[n+1,k] + \hat{H}_{12}^*[n,k]\, w_2[n,k] + \hat{H}_{22}[n,k]\, w_2^*[n+1,k] \\ \tilde{s}_2[n,k] &= \left(\left|\hat{H}_{11}[n,k]\right|^2 + \left|\hat{H}_{12}[n,k]\right|^2 + \left|\hat{H}_{21}[n,k]\right|^2 + \left|\hat{H}_{22}[n,k]\right|^2\right) s_2[n,k] + \hat{H}_{21}^*[n,k]\, w_1[n,k] - \\ &\quad \hat{H}_{11}[n,k]\, w_1^*[n+1,k] + \hat{H}_{22}^*[n,k]\, w_2[n,k] - \hat{H}_{12}[n,k]\, w_2^*[n+1,k] \end{aligned} \tag{3.12}$$

As seen in Equation (3.12), the estimates of the transmitted OFDM symbols mostly depend on the magnitudes of the channels and they are resistant to phase changes.

C. SUMMARY

In this chapter, we introduced multicarrier modulation and OFDM as a viable technique for efficient communication in frequency-selective channels. In particular, we have indicated that the use of multiple antennas in conjunction with STBC and MRC greatly improves the overall channel capacity. However, this is achieved under the condition that the channel is known at the receiver.

In the next chapter, we will discuss various channel estimation methods for systems employing receiver and/or transmitter diversity.

IV. CHANNEL ESTIMATION METHODS FOR OFDM SYSTEMS WITH SINGLE AND MULTIPLE TRANSMIT ANTENNAS

OFDM systems utilizing coherent phase-shift-keying require accurate channel state information at the receiver in order to decode the transmitted signals correctly. We can obtain and track the channel state information by using a channel estimator at the receiver.

Channel estimation methods can be divided into two groups. The first method is called *block-type* channel estimation where pilot tones are inserted in all of the OFDM sub-carriers as training signals for channel estimation [6]. After we get the initial state of the channel, a decision-directed algorithm must be used in order to track the channel variations. The second channel estimation method uses pilot tones inserted between data sub-carriers in each of the OFDM blocks and is called *comb-type* channel estimation [6].

Both channel estimation methods have their own advantages and disadvantages. They can use both time and frequency correlations of the channel but, for low complexity estimators, generally frequency correlation is utilized.

Channel estimation methods also show some difference between systems with a single-transmit antenna and systems with transmitter diversity. While the complexity of the estimators is low for systems with a single-transmit antenna, the estimators for systems with multiple transmitters are very complex. This high complexity stems from the fact that signals transmitted from multiple antennas interfere with each other at the receivers [7].

In this chapter, we discuss both block-type and comb-type low complexity channel estimation methods for OFDM systems with single and multiple transmit antennas.

A. CHANNEL ESTIMATION METHODS FOR OFDM SYSTEMS WITH A SINGLE-TRANSMIT ANTENNA

The channel estimation algorithms for SISO-OFDM systems and SIMO-OFDM systems share the same methodology. In this thesis, we addressed SIMO-OFDM systems,

but the techniques presented in this section can be applied to any OFDM system with a single-transmit antenna.

First we will discuss a block-type channel estimation method, which requires a decision-directed algorithm in order to track the channel variations. Subsequently, a comb-type channel estimation method for single-transmit antenna systems will be presented.

1. Block-Type Channel Estimation

Block-type channel estimation uses pilot tones inserted in all of the sub-carriers of an OFDM block. Since we discuss the single-transmit antenna case, by sending a training OFDM block consisting of pilot tones, we can get the initial estimate of the channel coefficients prior to data transmission. The single-transmit antenna OFDM system with channel estimator that we used in our simulations is shown in Figure 12. Although we used QPSK modulation, the estimation algorithms can be used with any other digital modulation scheme.

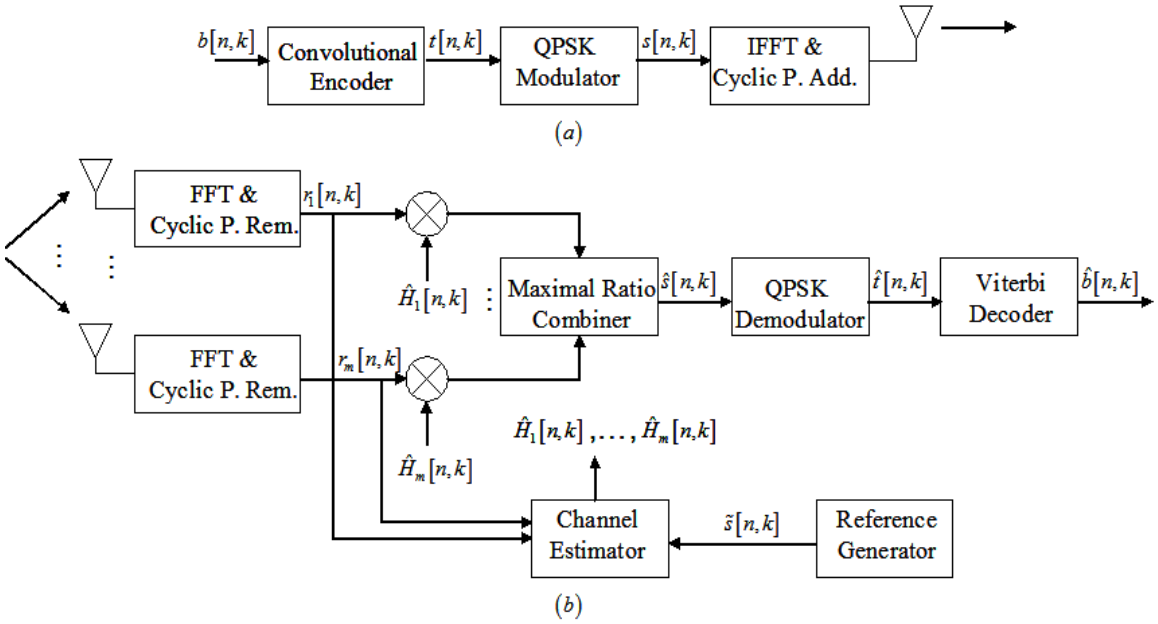

Figure 12. SIMO-OFDM system with block-type channel estimator (a) Transmitter (b) Receiver

In Figure 12, $b[n,k]$ represents the binary data before encoding, $t[n,k]$ is the binary data after encoding, $s[n,k]$ is the QPSK modulated signal before the IFFT

operation and $r_m[n,k]$ is the received signal after the FFT operation where *n* is the OFDM block index (time index), *k* is the OFDM sub-carrier (tone) index (frequency and sample index) and *m* is the receive antenna index. The correspondent received signal can be expressed as

$$r_m[n,k] = H_m[n,k]s[n,k] + w_m[n,k] \tag{4.1}$$

where $w_m[n,k]$ represents additive white Gaussian noise as explained in Chapter III. The frequency response of the channel between the transmit antenna and the m^{th} receive antenna at the n^{th} OFDM block and k^{th} tone is denoted as $H_m[n,k]$. The channel is assumed independent for different *m*'s but with the same statistics as defined in Chapter II. We perform channel estimation for each receive antenna independently.

a. Least-Square (LS) Channel Estimation

Channel estimation is based on standard LS techniques. We can write the transmitted and the received signals in vector form as

$$\begin{aligned} r[n] &= \left[r[n,0], r[n,1], ..., r[n,K-1] \right] \\ s[n] &= \left[s[n,0], s[n,1], ..., s[n,K-1] \right] \end{aligned} \tag{4.2}$$

where $r[n]$ and $s[n]$ are the vectors containing samples $r[n,k]$ and $s[n,k]$ respectively for $k = 0,1,...,K-1$, and *K* is the total number of sub-carriers in an OFDM symbol. By simply dividing $r[n,k]$ by $s[n,k]$ we get the frequency response of the channel plus some noise. In this way, we can express the estimated channel frequency response by [5]

$$\hat{H}[n,k] = \frac{r[n,k]}{s[n,k]}, \quad \text{for } k = 0,1,...,K-1 \tag{4.3}$$

Since the transmitted signal is QPSK with unit magnitude

$$\frac{1}{s[n,k]} = s^*[n,k]$$

and we can rewrite Equation (4.3) as

$$\hat{H}[n,k] = r[n,k]s^*[n,k], \quad \text{for } k = 0,1,...,K-1 \tag{4.4}$$

While implementing this estimation technique, the frequency responses of the channels corresponding to different OFDM blocks and sub-carriers are assumed to be

independent of each other. Consequently, none of the correlation properties of the channel is used and the estimation is based on a Gaussian channel model [5]. The block diagram of the LS channel estimator is shown in Figure 13.

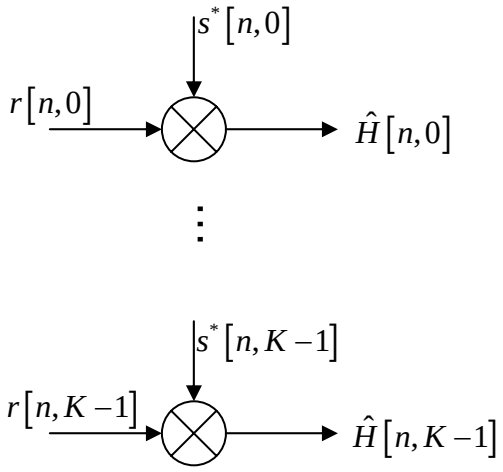

Figure 13. LS channel estimator

As seen in Equation (4.3), we need knowledge of the transmitted OFDM symbol in order to get the LS estimate of the channel frequency response. During the preliminary training period, we use symbols known at the receiver while during data transmission we use the reconstructed data symbols. We will discuss several reference generation methods at the end of this chapter.

b. Modified LS Channel Estimation

LS estimation methods have very low complexity, and they are easy to implement. The drawback of the LS estimator is a large mean-square-error (MSE). The modified LS estimator discussed here increases the performance of the LS estimator at the expense of higher complexity.

The LS estimation method presented in the previous subsection assumes independent components of the frequency response and does not use the correlation properties of the channel, thus making it sensitive to noise. The discrete samples of the impulse response are correlated in time up to the maximum time delay spread T_m of the channel. By using these time-domain statistics of the channel, we can improve the performance of the LS channel estimator for a wide range of SNRs [5].

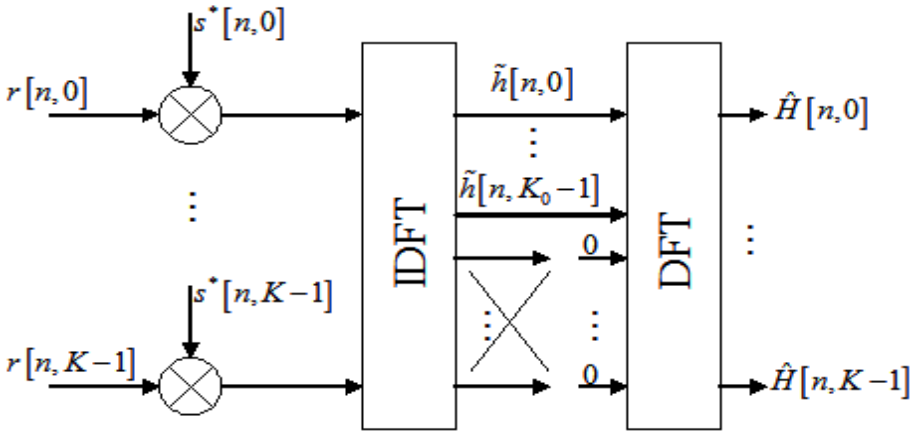

Figure 14. Modified LS channel estimator (After Ref. [5])

The modified LS channel estimator block diagram is shown in Figure 14. A temporal estimation of $H[n,k]$ is obtained as [3]

$$\tilde{H}[n,k] = r[n,k]s^*[n,k] = H[n,k] + w[n,k]s^*[n,k] \tag{4.5}$$

By taking the IDFT of $\tilde{H}[n,k]$, we obtain the channel impulse response $\tilde{h}[n,k]$ in the time-domain. The maximum delay spread of the channel impulse response is assumed to be less than the guard time interval to avoid ISI. Since this is known a priori, we can use this property to improve the performance of the channel estimator. By excluding low energy taps and using only the first K_0 taps of $\tilde{h}[n,k]$, we can eliminate some of the channel noise energy. The index K_0 depends on the channel delay profiles and can be taken as [3]

$$K_0 = \left\lceil \frac{KT_m}{T_s} \right\rceil \tag{4.6}$$

where K is the total number of tones in an OFDM symbol, T_m is the maximum delay spread of the channel and T_s is the OFDM symbol time. We can find the modified LS estimate of the channel frequency response by taking the K-point discrete Fourier transform (DFT) of $\tilde{h}[n,l]$, for $l = 0,1,...,K_0 - 1$. This is equivalent to padding the impulse response with $K - K_0$ zeros and then taking its DFT. In cases where we do not have any information about the delay profiles of the channel, we can use the length of the guard interval as a substitute for K_0.

By keeping the dominant components of the channel impulse response, we make the estimate less sensitive to noise. This stems from the fact that the noise is stationary, but the energy of the channel taps decrease rapidly after K_0 taps.

2. Comb-Type Channel Estimation for Systems with a Single Transmit Antenna

In comb-type channel estimation, which is also called pilot symbol aided channel estimation, we periodically insert pilot tones in the OFDM blocks and transmit them along with the data. Since we know the frequency response of the channel at the pilot inserted sub-carriers, we can obtain the whole channel frequency response by using an interpolation method. The block diagram of the comb-type channel estimator that we used for single-transmit antenna systems in our simulations is shown in Figure 15.

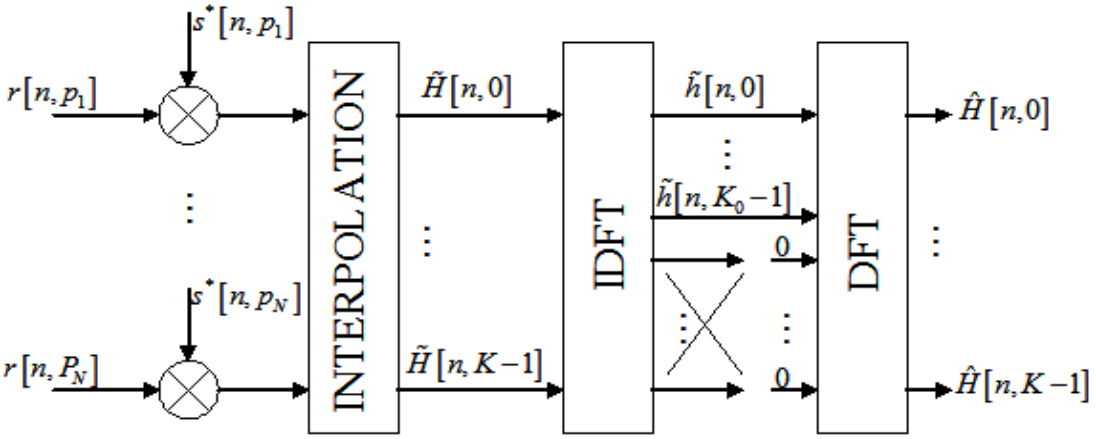

Figure 15. Comb-type channel estimator for single-transmit antenna systems

In Figure 15, $s[n,p]$ and $r[n,p]$ for $p = p_1,..., p_N$ are the transmitted and received pilot symbols at pilot position p, respectively, and N is the total number of pilot sub-carriers. First, the zero-forcing LS estimate of the frequency response of the channel at the pilot frequencies is found and an interpolation technique is then applied in order to get the whole channel frequency response. As a second step, as we have done in the modified LS estimation method, we take the IDFT of the frequency response found by interpolation and use a time-domain filter to exclude the taps greater than $K_0 - 1$ where K_0 depends on the channel delay profile. Finally, we take the DFT of the filtered impulse response and find the estimated frequency response of the channel. If a lower complexity estimator is desired, the output of the interpolator block can be used directly.

While designing a comb-type channel estimator, two important issues must be taken into account other than the estimation technique we use. The first one is the insertion of the pilot tones. It has been shown in [16] that the minimum number of pilot tones required to get a satisfactory estimation performance is equal to the maximum length of the channel impulse response, which is denoted as K_0. It has also been shown in [16] that the minimum MSE of the channel impulse response occurs when the pilot tones are uniformly spaced as

$$\left\{ p_i, p_i + \frac{K}{K_0}, ..., p_i + \frac{(K_0 - 1)K}{K_0} \right\} \tag{4.7}$$

where p_i denotes the frequency index of the initial pilot tone. Recently, it has been also been observed by [8] that cyclic spaced pilots perform better than equally spaced pilots. However, when the number of OFDM tones is high the difference in performance between the two schemes is negligible. As a consequence, in our simulations, we choose to use equally spaced pilots and the results will be shown in Chapter V.

The other important issue that must be considered is the interpolation method to be used [6]**.** It has been shown that the lowpass interpolation gives the best performance among other interpolation methods such as linear interpolation, second-order interpolation, spline cubic interpolation and time-domain interpolation. In our simulations, we use lowpass interpolation, which inserts zeros between estimates of the channel at pilot frequencies and applies a lowpass finite impulse response filter to the zero-padded sequence. In this way, the estimated values at the pilot frequencies stay the same while the MSE between the interpolated points and their actual values become minimal [6]. In the simulations presented, we use lowpass interpolation since it gives the best performance.

B. CHANNEL ESTIMATION METHODS FOR OFDM SYSTEMS WITH MULTIPLE TRANSMIT ANTENNAS

As explained previously, in the case of multiple transmit antennas, we need to develop a different channel estimation technique. This is due to the fact that the transmitted signals need to be diverse, so they can be separated at the receiver.

In this section, we will discuss the block-type and comb-type channel estimators for multiple-transmit antenna systems.

1. Block-Type Channel Estimation

As in the single-transmit antenna case, the channel estimation techniques that we discuss for multiple-transmit antenna systems are considered for each receive antenna independently. The block diagram of the OFDM system with transmitter and receiver diversity utilizing STBC with channel estimator is shown in Figure 16.

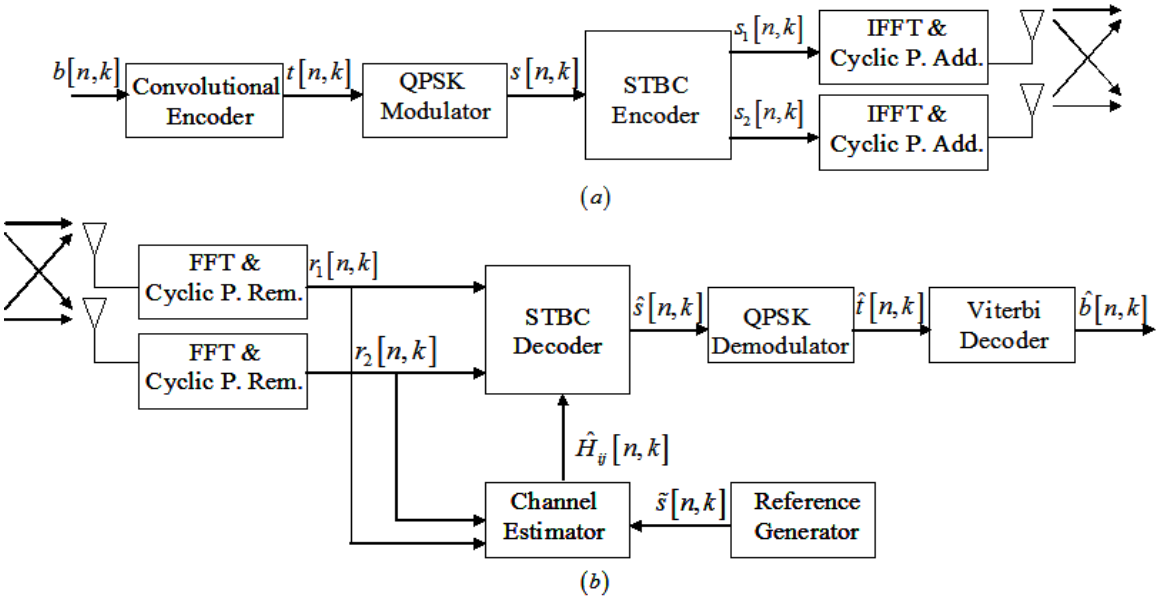

Figure 16. 2×2 MIMO-OFDM system with block-type channel estimator (a) Transmitter (b) Receiver

Since we use two transmit and two receive antennas, there will be a total of four different channels to be estimated. Denoting the frequency response of the channel between the i^{th} transmit antenna and the j^{th} receive antenna at the n^{th} OFDM block and the k^{th} sub-carrirer as $H_{ij}[n,k]$, the received signal at each antenna can be written as

$$r_j[n,k] = \sum_{i=1}^{2} H_{ij}[n,k]\, s_i[n,k] + w_j[n,k] \tag{4.8}$$

where $r_j[n,k]$, $s_i[n,k]$ are the received and the transmitted signals, respectively. Since we process the received signal at each antenna independently, we can leave out the receive antenna index and rewrite Equation (4.8) as

$$r[n,k] = \sum_{i=1}^{2} H_i[n,k]\, s_i[n,k] + w[n,k] \tag{4.9}$$

a. Basic Channel Estimation

As we have mentioned before, if we use block-type channel estimators the initial estimation of the channel coefficients requires transmitting training blocks. Since we also apply STBC to the transmitted symbols with the transmission sequence order as shown in Table 1 in Chapter III, we need to transmit at least two OFDM symbols as training blocks. Assuming that the first two blocks are known at the receiver, the estimated channel frequency response or impulse response can be obtained by using the frequency correlation of the channel parameters and minimizing the LS cost function [7]

$$\begin{aligned} C\left\{\hat{H}_i[n,k];\ i=1,2\right\} &= \sum_{k=0}^{K-1}\left| r[n,k]-\sum_{i=1}^{2}\hat{H}_i[n,k]s_i[n,k]\right|^2 \\ &= \sum_{k=0}^{K-1}\left| r[n,k]-\sum_{i=1}^{2}\sum_{l=0}^{K_0-1}\hat{h}_i[n,k]s_i[n,k]e^{-j2\pi kl/K}\right|^2 \end{aligned} \tag{4.10}$$

where K_0 depends on the channel delay profiles. When Equation (4.10) is minimized, we obtain

$$\sum_{k=0}^{K-1}\left(r[n,k]-\sum_{i=1}^{2}\sum_{l=0}^{K_0-1}\hat{h}_i[n,l]s_i[n,k]e^{-j2\pi kl/K}\right)s_m^*[n,k]e^{j2\pi kl_0/K}=0 \tag{4.11}$$

for $m=1,2$ and $l_0=0,1,...,K_0-1$. Equation (4.11) can be rewritten as

$$\sum_{k=0}^{K-1} r[n,k]s_m^*[n,k]e^{j2\pi kl_0/K}=\sum_{i=1}^{2}\sum_{l=0}^{K_0-1}\sum_{k=0}^{K-1}\hat{h}_i[n,l]s_i[n,k]s_m^*[n,k]e^{-j2\pi k(l-l_0)/K} \tag{4.12}$$

By defining

$$\begin{aligned} p_m[n,l] &= \sum_{k=0}^{K-1} r[n,k]s_m^*[n,k]e^{j2\pi kl/K} \\ q_{im}[n,l] &= \sum_{k=0}^{K-1} s_i[n,k]s_m^*[n,k]e^{j2\pi kl/K} \end{aligned} \tag{4.13}$$

Equation (4.12) becomes

$$\sum_{i=1}^{2}\sum_{l=0}^{K_0-1}\hat{h}[n,l]q_{im}[n,l_0-l]=p_m[n,l_0] \tag{4.14}$$

Leaving the estimated channel impulse responses column vector $\hat{h}[n]$ alone and writing Equation (4.14) in matrix form, we get [7]

$$\hat{h}[n]=Q^{-1}[n]\,p[n] \tag{4.15}$$

where

$$\hat{h}[n]=\begin{pmatrix}\hat{h}_1[n]\\ \hat{h}_2[n]\end{pmatrix},$$

$$\hat{h}_i[n]=\left[\hat{h}_i[n,0],\hat{h}_i[n,1],...,\hat{h}_i[n,K_0-1]\right]^T$$

$$p[n]=\begin{pmatrix}p_1[n]\\ p_2[n]\end{pmatrix},$$

$$p_i[n]=\left[p_i[n,0],p_i[n,1],...,p_i[n,K_0-1]\right]^T$$

$$Q[n]=\begin{pmatrix}Q_{11}[n] & Q_{21}[n]\\ Q_{12}[n] & Q_{22}[n]\end{pmatrix},$$

$$Q_{im}[n]=\begin{pmatrix}q_{im}[n,0] & q_{im}[n,-1] & \cdots & q_{im}[n,-K_0+1]\\ q_{im}[n,1] & q_{im}[n,2] & \cdots & q_{im}[n,-K_0+2]\\ \vdots & \ddots & \ddots & \vdots\\ q_{im}[n,K_0-1] & q_{im}[n,K_0-2] & \cdots & q_{im}[n,0]\end{pmatrix},\ \text{for } i,m=1,2$$

In Equation (4.15), we can obtain $q_{im}[n,-l]$ by symmetry, as

$$q_{im}[n,-l]=q_{im}[n,K-l] \tag{4.16}$$

As we determined the channel impulse responses, we compute the frequency responses of the channels by using the DFT. The block diagram of the basic channel estimator is shown in Figure 17.

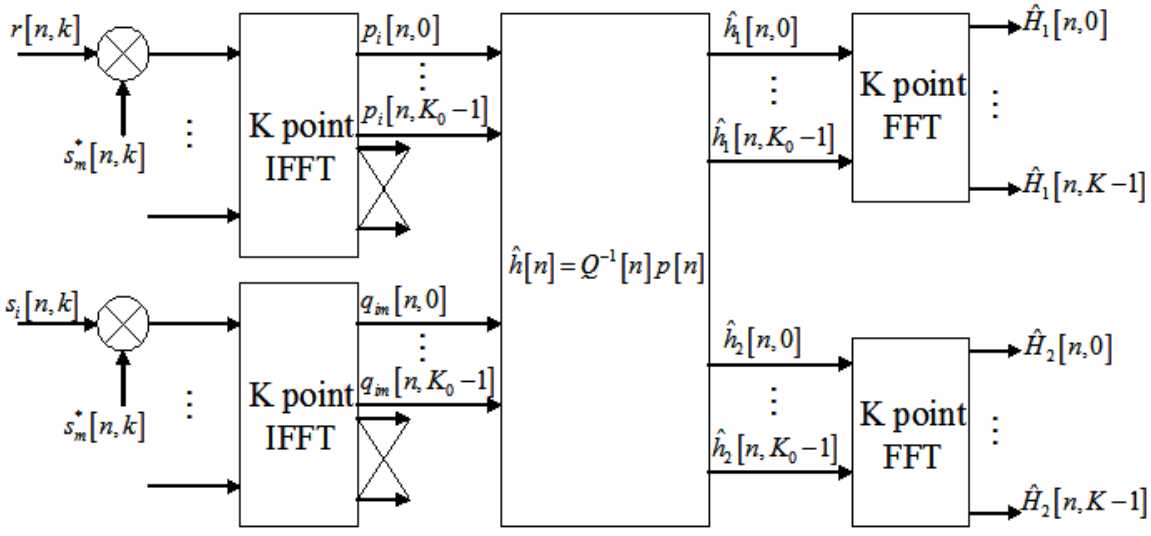

Figure 17. Basic block-type channel estimator for OFDM systems with transmitter diversity (After Ref. [7])

b. Channel Estimation with Significant Tap Catching (STC) Method

As seen in Equation (4.15), channel estimation requires a matrix inversion. In cases where the value of K_0 is large or we do not have any knowledge about the channel and use the length of the cyclic prefix as a substitute for K_0, the computation of this matrix inversion could be a heavy task for the channel estimator.

Fortunately in most cases, the channel impulse response has only a few significant values and we can use this fact to simplify the computations [7, 17].

If $\hat{h}_i[n,l]$ for $i=1,2$ and $l=0,1,...,K_0-1$ is the estimated impulse response of the channel during the training period, then the S most significant taps of the channel can be chosen by calculating

$$\sum_{l=0}^{K_0-1}\left|h_i[n,l]\right|^2 \tag{4.17}$$

and finding the indexes "l" corresponding to large energy. The significant taps indexes $0 \le l_1 < l_2 < ... < l_S \le K_0 - 1$ can be determined and Equation (4.15) becomes [7]

$$\bar{h}[n] = \bar{Q}^{-1}[n]\,\bar{p}[n] \tag{4.18}$$

where

$$\bar{h}[n] = \begin{pmatrix} \bar{h}_1[n] \\ \bar{h}_2[n] \end{pmatrix},$$

$$\bar{h}_i[n] = \left[\hat{h}_i[n,l_1], \hat{h}_i[n,1_2], ..., \hat{h}_i[n,l_S]\right]^T$$

$$\bar{p}[n] = \begin{pmatrix} \bar{p}_1[n] \\ \bar{p}_2[n] \end{pmatrix},$$

$$\bar{p}_i[n] = \left[p_i[n,l_1], p_i[n,1_2], ..., p_i[n,l_S]\right]^T$$

$$\bar{Q}[n] = \begin{pmatrix} \bar{Q}_{11}[n] & \bar{Q}_{21}[n] \\ \bar{Q}_{12}[n] & \bar{Q}_{22}[n] \end{pmatrix},$$

$$\bar{Q}_{im}[n] = \begin{pmatrix} q_{im}[n,0] & q_{im}[n,l_1-l_2] & \dots & q_{im}[n,l_1-l_S] \\ q_{im}[n,l_2-l_1] & q_{im}[n,0] & \dots & q_{im}[n,l_2-l_S] \\ \vdots & \ddots & \ddots & \vdots \\ q_{im}[n,l_S-l_1] & q_{im}[n,l_S-l_2] & \dots & q_{im}[n,0] \end{pmatrix}, \text{ for } i,m=1,2$$

Since $\bar{h}_i[n]$ is the column vector containing the gains of the significant taps, the estimated time-domain channel impulse response can be found by keeping the significant taps' gains and setting to zero the less significant ones. The estimated frequency response of the channel can then be computed as

$$\bar{H}_i[n,k] = \sum_{s=1}^{S} \bar{h}_i[n,l_s] e^{-j2\pi k l_s / K} \tag{4.19}$$

The choice of the number of significant taps *S* depends on the multipath environment, the desired computational complexity and the desired performance of the system. For channels with a large number of taps with significant energy, choosing a small value for *S* would cause poor performance whereas for channels with a small number of taps with significant energy choosing a large number for *S* would cause the system to be more sensitive to channel noise due to their small SNR.

c. Optimum Training Symbol Design and Simplified Channel Estimation

In the previous subsection, it has been shown that the computational complexity of the estimator could be reduced by using the STC approach. However, the $\bar{Q}$ matrix in Equation (4.18) still has to be inverted. This causes a problem for a channel with a large number of taps with significant energy.

If all the sub-carriers of the OFDM system are used for symbol transmission without using any null carriers, then it is possible to design training symbols in such a way that the estimator does not require any matrix inversion operation during the training period.

It has been shown in [7, 9] that optimum training symbols, which do not require any matrix inversion, can be designed by choosing

$$\begin{aligned} s_1[n] &= [a_0, a_1, a_2, ..., a_{K-1}] \\ s_2[n] &= [a_0, -a_1, a_2 ..., -a_{K-1}] \end{aligned} \tag{4.20}$$

where $s_1[n]$ and $s_2[n]$ are the output signals of the STBC encoder block and a_k for $k = 0,1,...,K-1$ are complex numbers with magnitude 1.

In this case, $Q_{ii}[n] = K\mathrm{I}$ for $i = 1, 2$, where I represents the $K_0 \times K_0$ identity matrix and K represents the total number of sub-carriers. This is the result of using training tones with magnitude 1. The design using the optimum training symbols yields $Q_{im}[n] = \mathbf{0}$ for $i, m = 1, 2$ and $i \neq m$ where $\mathbf{0}$ represents a $K_0 \times K_0$ matrix of zeros. Then, we can obtain the estimated channel impulse responses by [9]

$$\hat{h}_i[n, l] = \frac{1}{K} p_i[n, l] \text{ for } l = 0, 1, ..., K_0 - 1 \tag{4.21}$$

without the need of a matrix inversion.

It has also been shown in [7] that the design of optimum training symbols yields slightly better performance than any other training symbols, with considerably reduced computational complexity.

During the data transmission, the complexity of the estimator is still high and we need to find an efficient way to update the channel estimation. In this case, we make use of the previously estimated channel coefficients. We can write Equation (4.15) as

$$\begin{aligned} Q_{11}[n]\hat{h}_1[n] &= p_1[n] - Q_{21}[n]\hat{h}_2[n] \\ Q_{22}[n]\hat{h}_2[n] &= p_2[n] - Q_{12}[n]\hat{h}_1[n] \end{aligned} \tag{4.22}$$

In particular $Q_{ii}[n] = K\mathrm{I}$ for $i = 1, 2$ and Equation (4.22) can be rewritten as

$$\begin{aligned} \hat{h}_1[n] &= \frac{1}{K}\left(p_1[n] - Q_{21}[n]\hat{h}_2[n]\right) \\ \hat{h}_2[n] &= \frac{1}{K}\left(p_2[n] - Q_{12}[n]\hat{h}_1[n]\right) \end{aligned} \tag{4.23}$$

Equation (4.23) shows that if we have one of the estimated impulse responses then we can get the other one without using any matrix inversion. In [9], it has been proposed that we could use previously estimated channel impulse responses $\hat{h}_1[n-1]$ and $\hat{h}_2[n-1]$ to substitute $\hat{h}_1[n]$ and $\hat{h}_2[n]$ respectively and compute the current estimates as

$$\hat{h}_1[n] = \frac{1}{K}\left(p_1[n] - Q_{21}[n]\hat{h}_2[n-1]\right)$$
$$\hat{h}_2[n] = \frac{1}{K}\left(p_2[n] - Q_{12}[n]\hat{h}_1[n-1]\right) \quad (4.24)$$

Since we use the previously estimated values to obtain the current estimates of the channel impulse responses, this could cause some performance degradation when the channel has a high Doppler frequency. By periodically inserting training symbols, this problem can be solved. The simulation results will be presented in Chapter V.

The STC method can also be combined with the simplified channel estimation in order to reduce the complexity of the channel estimator.

It should be noted again that Equations (4.23) and (4.24) are true under the assumptions that the transmitted data tones have magnitude of 1, and all of the sub-carriers are used for data transmission.

2. Comb-Type Channel Estimation for Systems with Multiple Transmit Antennas

By writing the LS cost function in Equation (4.10) in matrix form we get

$$C\left\{\hat{H}_i[n,k];\ i=1,2\right\} = \left(R - S_1\hat{H}_1 - S_2\hat{H}_2\right)^H \left(R - S_1\hat{H}_1 - S_2\hat{H}_2\right) \quad (4.25)$$

where $(.)^H$ denotes Hermitian transpose and R, S_i and $\hat{H}_i$ for $i = 1, 2$ are the matrix form representations with the elements from the received signal $r[n]$, transmitted signals $s_i[n]$ for $i = 1, 2$ and estimated frequency responses $\hat{H}_i[n]$ for $i = 1, 2$ on their diagonals respectively. When the LS cost function is minimized, we obtain the equation

$$-S_1^H R + S_1^H S_1\hat{H}_1 + S_1^H S_2\hat{H}_2 = 0$$
$$-S_2^H R + S_2^H S_2\hat{H}_2 + S_2^H S_1\hat{H}_1 = 0 \quad (4.26)$$

where $R = S_1H_1 + S_2H_2$ for the noiseless case. Choosing $S_1^H S_2 = 0$ and $S_2^H S_1 = 0$ and by using optimum training symbols in block-type estimation, we can obtain the estimates of the channel frequency responses simply by [8]

$$\hat{H}_1 = \left(S_1^H S_1\right)^{-1} S_1^H R$$
$$\hat{H}_2 = \left(S_2^H S_2\right)^{-1} S_2^H R \quad (4.27)$$

Using the optimum training symbols described above, we can generate a comb-type channel estimation method which avoids transmit antenna interference at the receiver. So, by choosing [8]

$$\begin{aligned} s_1\left[n_p, k_p\right] &\neq 0 \text{ when } s_2\left[n_p, k_p\right] = 0 \\ s_1\left[n_p, k_p\right] &= 0 \text{ when } s_2\left[n_p, k_p\right] \neq 0 \end{aligned} \tag{4.28}$$

where n_p and k_p denote the symbol index and sub-carrier index of the pilot tone inserted OFDM symbol, we can implement a comb-type estimation for transmitter diversity systems that use the same low-complexity algorithm mentioned in the single-transmit antenna case. We can call this an optimum pilot tone design.

Since we use STBC in our OFDM system, which utilizes a symmetric data transmission algorithm in time, the pilot insertion must be as shown in Table 2.

OFDM block	Transmit Antenna-1	Transmit Antenna-2
n_p	$s_2\left[n_p, k_p\right] = 0$	$s_2\left[n_p, k_p\right] = 0$
$n_p + 1$	$s_1\left[n_p + 1, k_p\right] = 0$	$s_2[n_p + 1, k_p] = s_1^*[n_p, k_p]$

Table 2. Pilot insertion for STBC-OFDM utilizing comb-type channel estimation method

Other than the optimum pilot design and pilot insertion arrangement, the estimator follows the same methodology as explained for single-transmit antenna systems. The pilot insertion arrangement and density that we use in our simulations will be shown in Chapter V.

C. REFERENCE GENERATION

As it has been explained in the previous sections, we need to generate references of the transmitted symbols for systems using block-type channel estimators, in order to track the channel variations in time and frequency. The transmitted symbol reference can be generated by using various reference generation methods as it has been shown in [3]. We use three different reference generation methods and their structures are shown in Figure 18.

The *decoded reference* is generated by using the estimated binary data of the previous OFDM symbol as shown in Figure 18a. As we have a reference symbol, we can use it to estimate the channel coefficients of the previous OFDM block. If the output of the Viterbi decoder does not give the original transmitted data, then using this reference generation method will cause error propagation to the estimation process of the consecutive OFDM symbols. Since we estimate the previous OFDM block's channel coefficients and use it to decode the current OFDM symbol while the channel changes with time, this will also cause a significant error when the channel's Doppler frequency spread is large. In order to reduce the error propagation in the estimation of the consecutive OFDM symbols, instead of only using training blocks at the beginning of the transmission, we can send training blocks periodically. If we choose to use this reference generation method, then, except the training block transmissions, the estimated frequency response of the previous OFDM block is used as $\hat{H}[n,k]$ as shown in Figures 12 and 16.

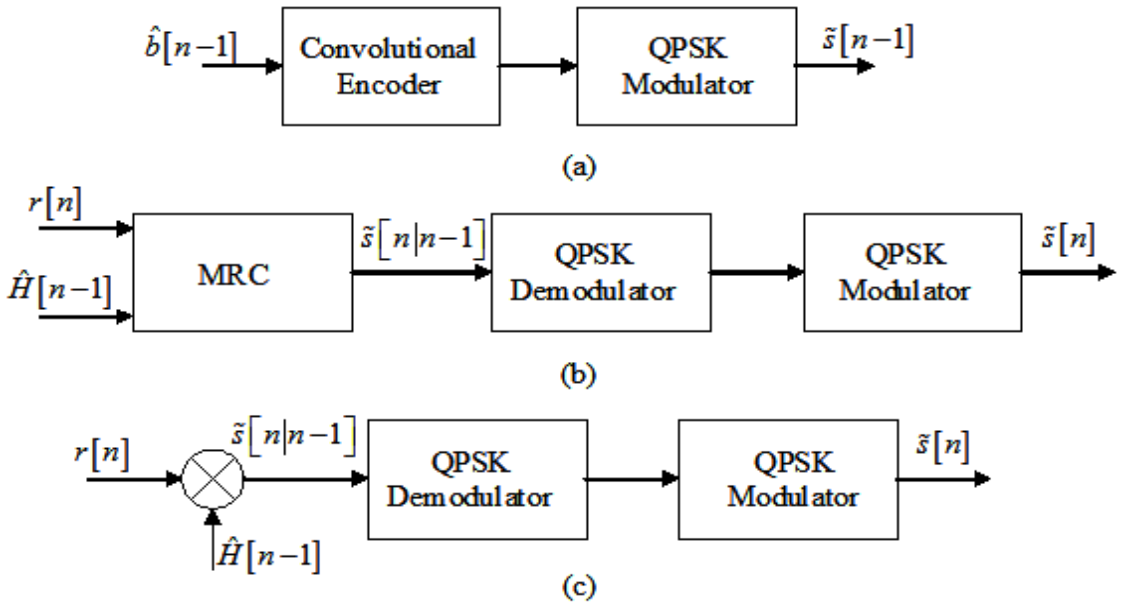

Figure 18. Reference generation (a) Decoded reference (b) Undecoded reference (c) Zero-forcing reference

The *undecoded reference* can be generated as shown in Figure 18b. First, we determine a predicted estimate $\tilde{s}[n|n-1]$ of the transmitted symbol $s[n]$ using the available channel estimate $\hat{H}[n-1]$. Then we update the estimate of the channel $\hat{H}[n]$ by

using $\hat{s}\left[n|n-1\right]$ and use $\hat{H}\left[n\right]$ to obtain the updated decision of the transmitted symbol $\tilde{s}\left[n\right]$. This method is more complex than the decoded reference generation method. For multiple-transmit antenna systems, which we use in our simulations, instead of applying an additional MRC operation an additional STBC operation is performed.

The *zero-forcing reference* can be used with single-transmit antenna systems only since we need the received symbols with no interference to be able to generate the appropriate reference. Its complexity is lower than the decoded and the undecoded reference methods. We obtain a predicted LS estimate $\tilde{s}\left[n|n-1\right]$ of the transmitted symbol by using the available channel estimate $\hat{H}\left[n-1\right]$ as shown in Figure 18c. Subsequently, decision feedback is applied to obtain $\tilde{s}\left[n\right]$ and then the channel coefficients are updated.

The performances of channel estimators using these reference generation methods will be shown in Chapter V.

D. SUMMARY

In this chapter, first we discussed low complexity block-type and comb-type channel estimation techniques for SIMO-OFDM systems utilizing MRC and explained the main differences between block-type and comb-type channel estimators. Subsequently, we discussed the block-type and the comb-type channel estimation algorithms for OFDM systems utilizing STBC and presented the differences between estimation techniques for multiple and single-transmit antenna systems. As the last step, we presented three reference generation methods, which we need in order to track the channel variations, with different complexities for block-type channel estimators.

In the next chapter, we will discuss the simulation model developed to study the various channel estimation methods explained in this chapter and present the simulation results obtained.

THIS PAGE INTENTIONALLY LEFT BLANK

V. SIMULATION RESULTS

In this chapter, we present the simulation results of SIMO and MIMO-OFDM communication systems utilizing the channel estimation methods discussed in the previous chapter. The communication systems were developed using Matlab, and BER versus SNR curves were generated to evaluate the performances of the systems. For each SNR value, 1,200,000 bits were transmitted and Monte Carlo runs for all SNR values were conducted with new channel coefficients and new symbols at each run.

First, we will give the OFDM systems' parameters used in the simulations and subsequently present the simulation results.

A. OFDM SYSTEM PARAMETERS

The entire channel bandwidth W of the OFDM system and the sampling rate f_s were both chosen as 800 kHz. The total number of sub-carriers K was set to 128, which yielded the sub-carrier spacing

$$\Delta f = \frac{f_s}{K} = 6.25 \text{ kHz} \tag{5.1}$$

As a consequence, the OFDM symbol time was computed as

$$T_s = \frac{1}{\Delta f} = \frac{K}{f_s} = 160\mu s \tag{5.2}$$

In our simulations, we used a guard interval ratio of $\frac{1}{4}$, which yielded a guard interval of $40\mu s$. The total OFDM block time then became

$$T_b = T_s + T_g = 200\mu s \tag{5.3}$$

B. PERFORMANCE EVALUATION OF SIMULATED SYSTEMS

In this thesis, all the simulated systems used QPSK with the convolutional encoder described in Chapter III. Perfect synchronization between the transmitters and the receivers was assumed. We also assumed that the channel is quasi-static during one OFDM block transmission. The maximum delay spread of the channel T_m was simulated as $20\mu s$, which would not cause ISI, since it was smaller than the guard interval. In all simulations, we assumed that maximum delay spread of the channel was known a priori at the receiver.

The average SNR per OFDM block was computed by

$$\frac{S}{N} = \frac{\sum_{k=0}^{K+m-1} \left| r[n,k] \right|^2}{\rho^2} \tag{5.4}$$

where S is the received signal power, N is the noise power, $r[n,k]$ is the received signal, K is the total number of sub-carriers, m is the number of the guard samples and ρ is the variance of the additive white Gaussian noise. For accuracy, ρ was calculated for every received signal separately since the received signal energy might vary with time.

1. Performance of SIMO-OFDM Systems Utilizing Channel Estimation Methods

In the simulations, we use 120 sub-channels to transmit data and 4 sub-channels on each end as guard tones, also called null tones, in order to mitigate interference within adjacent channels. This structure results in a data rate of 600 kbits/s with coding and a transmission efficiency of 0.75 bits/s/Hz including the training symbol transmissions. The parameters for the simulations of the SIMO-OFDM (1×2) systems utilizing the block-type channel estimation methods are given in Table 3. Without the training symbols, the information data rate can be calculated as 525 kbits/s for a training symbol usage of 12.5%.

# of transmitted bits for each SNR	1,200,000
# of OFDM symbols transmitted for each SNR	10,000
# of Monte Carlo runs	10
% of OFDM symbols used as training	12.5%

Table 3. Parameters for simulations of the OFDM systems utilizing modified LS and LS estimation methods

Figure 19 shows the BER performances of the SIMO-OFDM systems using the modified LS channel estimator with various reference generation schemes. The simulation is performed over the typical urban area (TU) delay profile channel with Doppler frequency $f_d = 40$ Hz. Every eight OFDM symbols, one training symbol is transmitted for channel estimation and reference generation methods are used in order to estimate the channels' coefficients at subsequently transmitted OFDM blocks.

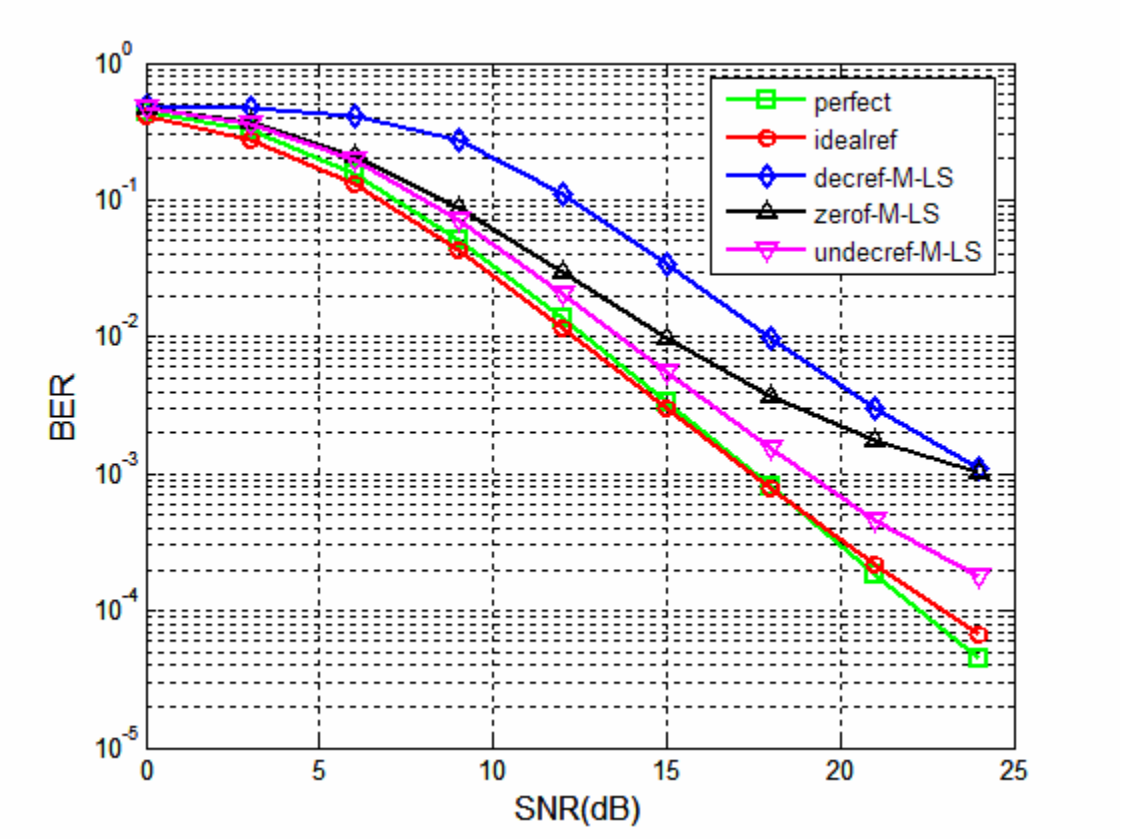

Figure 19. BER comparison of various reference generation schemes used with the modified LS estimator over the TU delay profile channel with $f_d = 40$ Hz

As seen in Figure 19, with modified LS channel estimator utilizing the ideal references, we get BER performance similar to the one we would have with perfect channel knowledge. The undecoded reference performs better than the decoded reference and the zero-forcing reference for all SNR values. Also, zero-forcing reference performs better than the decoded reference for a wide range of SNRs, but the difference between performances of these reference generation methods gets smaller as the SNR value increases. Since the undecoded and the zero-forcing reference generation methods use a predictor before obtaining the actual estimates of the channel coefficients, they perform better than the decoded reference generation method. As the SNR value increases, the error propagation of the decoded reference decreases and it begins to perform better. For a BER of 10^{-2}, the system utilizing the undecoded reference generation method performs 1.5 dB and 4.5 dB better than the systems utilizing the zero-forcing and the decoded reference generation methods, respectively, over the TU delay profile channels.

Figure 20 shows the BER comparison of SIMO-OFDM systems utilizing the modified LS and the LS channel estimators over the TU delay profile channel with $f_d = 40$ Hz. We use the undecoded reference since it gives the best performance among the other reference generation schemes.

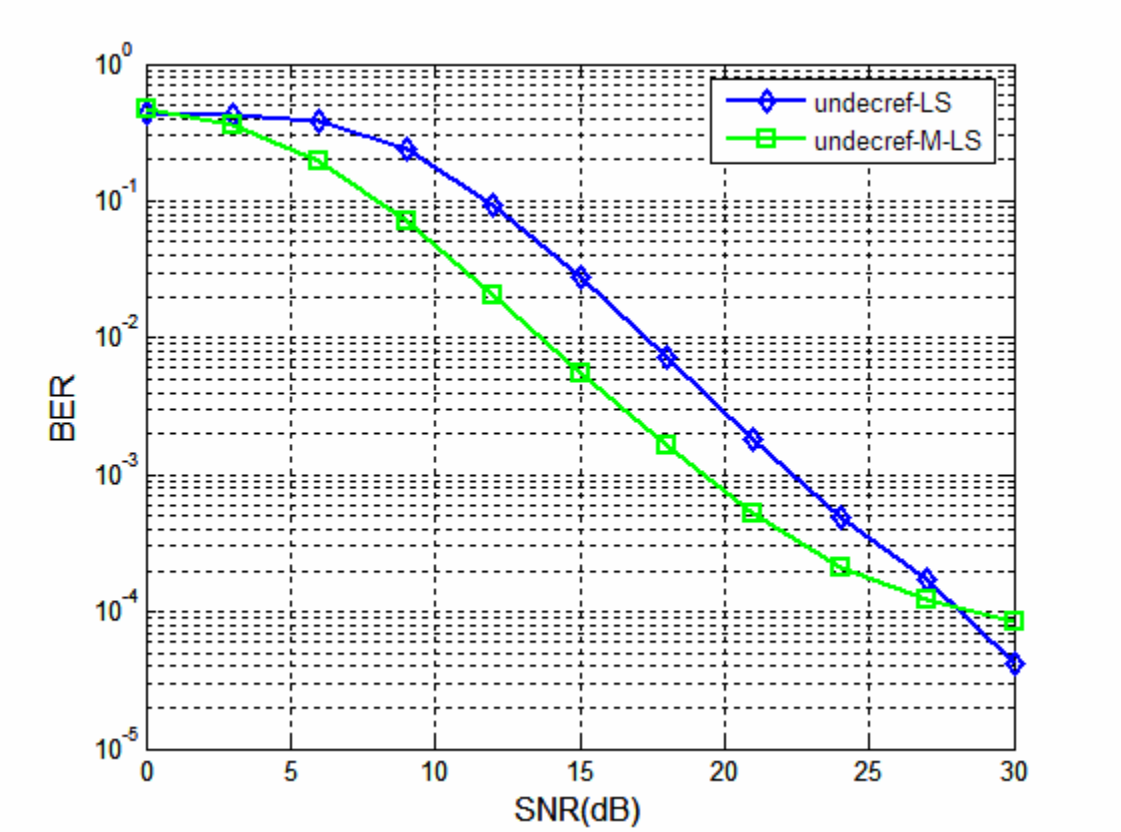

Figure 20. BER comparison of the modified LS estimator and the LS estimator over the TU delay profile channel with $f_d = 40$ Hz

As expected, the performance of the LS channel estimator gets better than the modified LS estimator at higher SNRs. This is due to the fact that the noise power becomes very small compared to the received signal power as the SNR increases. In high SNR, by eliminating some taps in the modified LS estimator case, we lose mostly signal energy rather than the noise energy. However, the modified LS estimator still performs better than the LS estimator for a long range of SNRs. For a BER of 10^{-2}, the modified LS estimator performs 3.5 dB better than the LS estimator over this specific channel.

Figure 21 also shows the BER comparison of the modified LS estimator and the LS estimator but this time over the hilly terrain (HT) delay profile channel with $f_d = 40$ Hz.

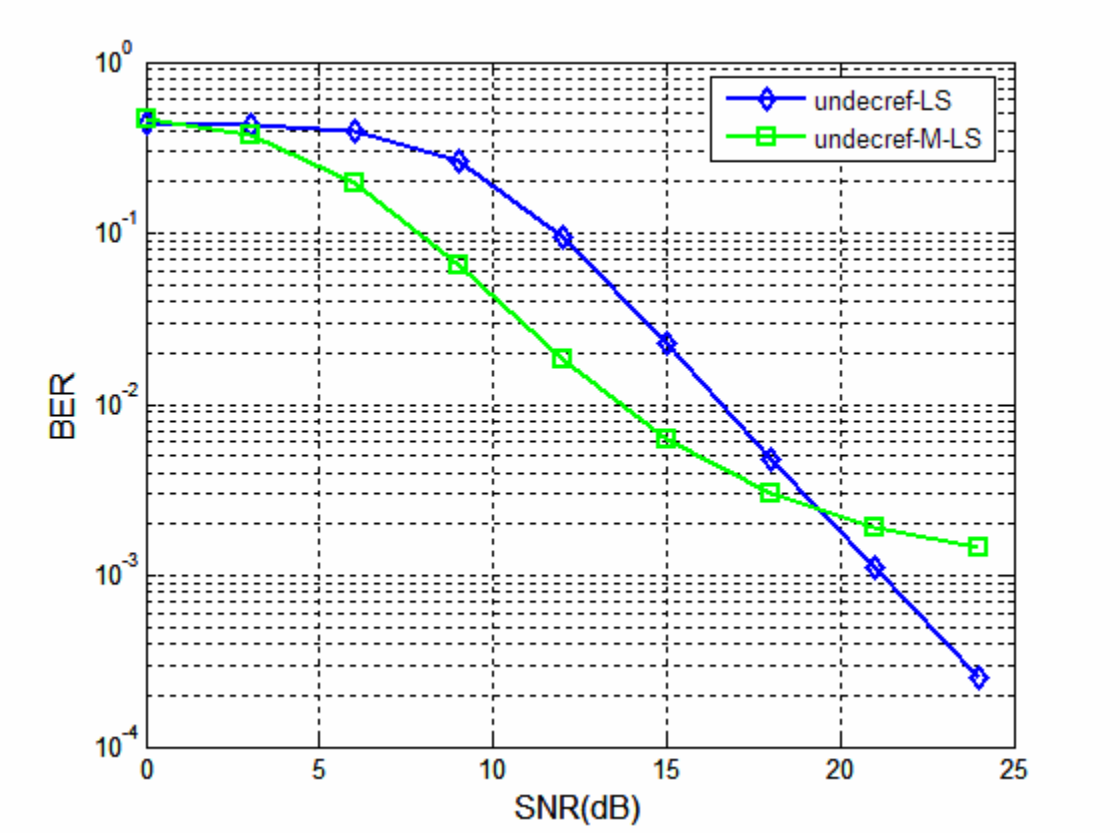

Figure 21. BER comparison of the modified LS estimator and the LS estimator over the HT delay profile channel with $f_d = 40$ Hz

Over the HT delay profile channel, the LS estimator begins to perform better than the modified LS estimator at a lower SNR value than it does over the TU delay profile channel. The modified LS estimator performs better than the LS estimator up to an SNR value of 19 dB. We can see that modified LS estimator's performance over the HT delay profile channel is worse than its performance over the TU delay profile channel.

For a SIMO-OFDM system utilizing comb-type channel estimation method, the pilot positions are chosen as $[5,9,13,...,121]$. The estimated frequency responses of the channels will have larger interpolation errors at the edge frequencies.

For the comb-type channel estimation method, we inserted pilot tones in each OFDM symbol to be transmitted. There are totally 30 pilot tones out of 120 information tones. This structure results in an information data rate of 450 Kbits/s. For simulations that compare the performances of both types of channel estimators, in order to make a fair comparison, we transmit one training OFDM block for every 4 symbol transmissions so that both methods satisfy the same information data rate.

In order to compare with the comb-type channel estimation method, we use the modified LS channel estimation technique as the block-type channel estimation algorithm. The parameters for the simulations of the SIMO-OFDM systems utilizing block-type and comb-type channel estimation methods are given in Table 4.

# of transmitted bits for each SNR	1,200,000
# of OFDM symbols transmitted for each SNR	10,000
# of Monte Carlo runs	10
% of OFDM symbols used as training	25%

Table 4. Parameters for simulations of the OFDM systems utilizing block-type and comb-type channel estimation methods

We also examine the performances of both types of channel estimation techniques at various Doppler frequencies. Figure 22 shows the performance of the modified LS channel estimation method using undecoded reference over the TU delay profile channel with various Doppler frequencies. As the Doppler frequency increases, the performance of the modified LS estimator decreases. For low SNR values, the difference between the performances of the system at three different Doppler frequencies is not very large. For a Doppler frequency of 200 Hz, the performance increment of the modified LS estimator gets slower as the SNR increases. We can also see that the modified channel estimator performs much better over an additive white Gaussian noise (AWGN) channel.

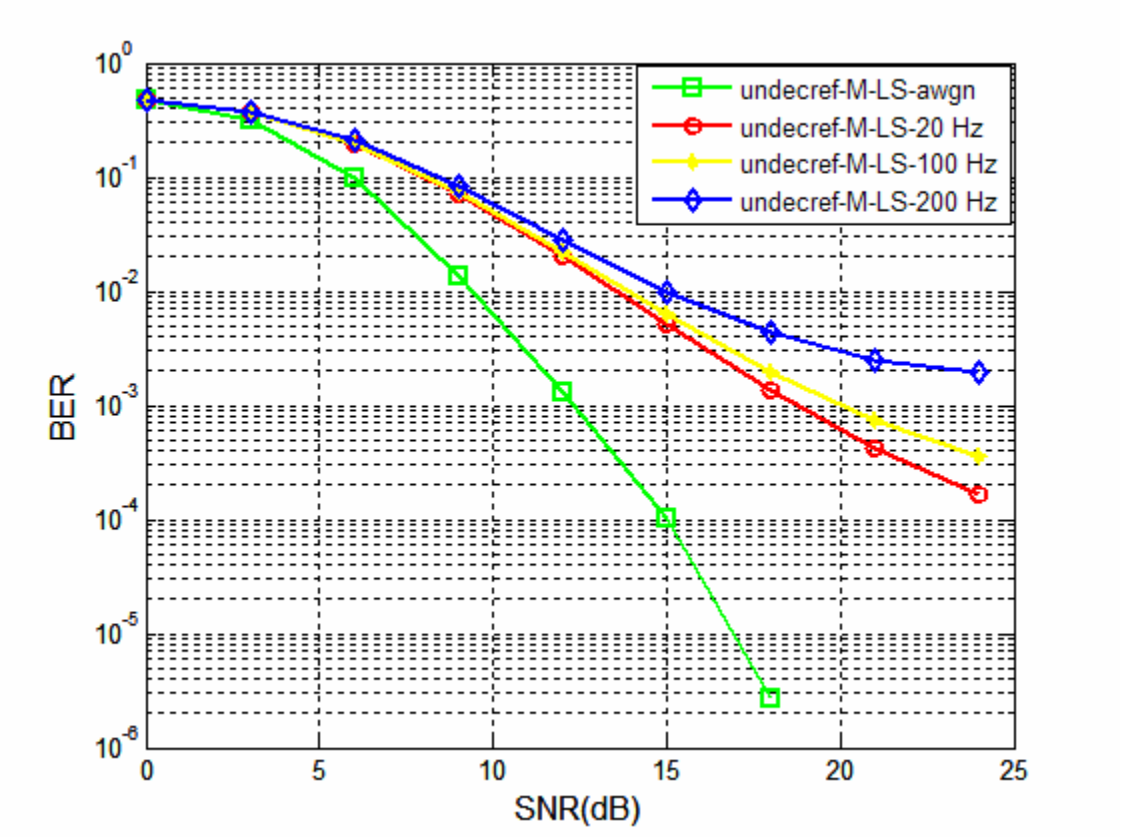

Figure 22. BER comparison of the modified LS estimator at various Doppler frequencies over the TU delay profile channel

Figure 23 shows the BER performance of the comb-type channel estimation method utilizing the lowpass interpolation over the TU delay profile channel with various Doppler frequencies. We see that the performance of the comb-type channel estimator is also much better over an AWGN channel than its performances over the TU delay profile channels with various Doppler frequencies. For the comb-type channel estimator, the BER performance does not change considerably as the Doppler frequency increases. For low SNRs, the performance of the estimator is almost the same for all three Doppler frequencies. As the SNR increases, we begin to see that the performance of the estimator degrades slightly. In the comb-type channel estimation method, we insert pilot tones known at the receiver in each OFDM block and perform channel estimation using these pilot tones. Unlike the block-type channel estimation algorithm, in the comb-type channel estimation method, we do not use any data related to the previously transmitted OFDM blocks. This is the reason why the performance of the comb-type channel estimator does

not degrade as much as the performance of the modified LS channel estimator as the Doppler frequency of the channel increases. For the comb-type channel estimation technique, the main source of the estimation error is due to interpolation.

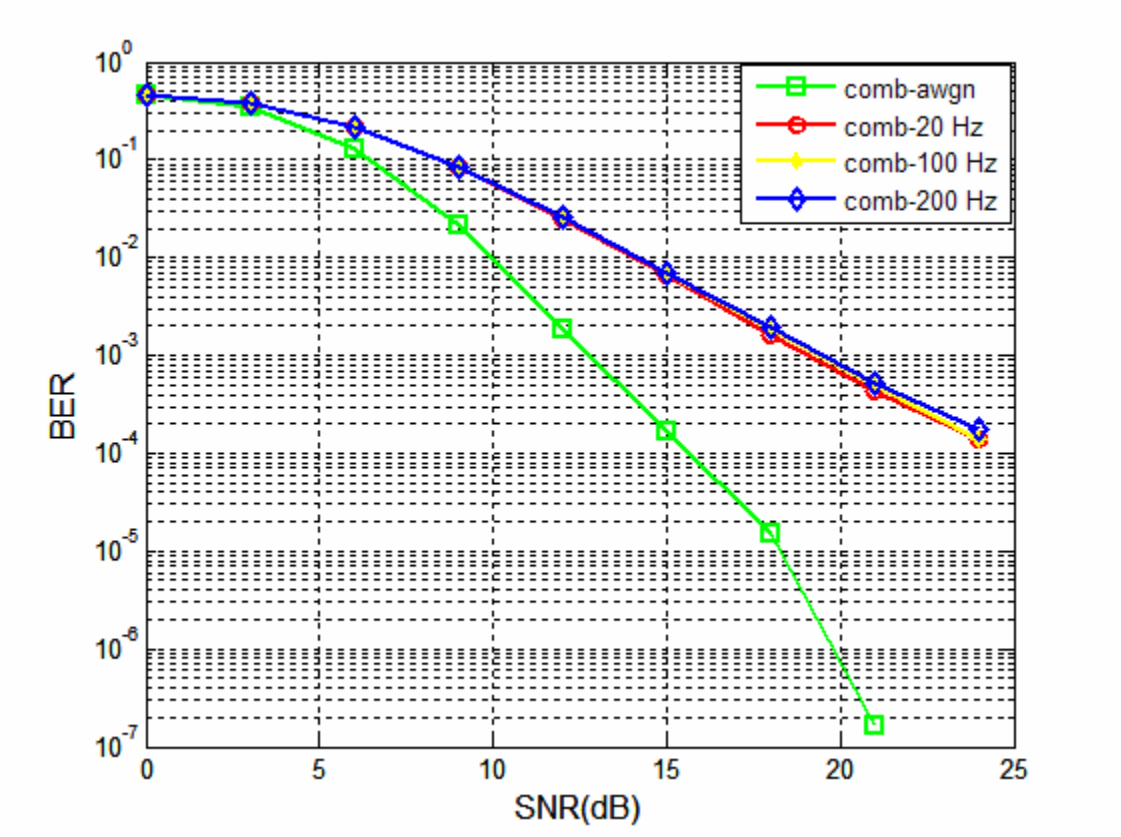

Figure 23. BER comparison of the comb-type channel estimator at various Doppler frequencies over the TU delay profile channel

In Figure 24, we show the performances of both types of channel estimators over the TU delay profile channel with $f_d = 20$ Hz and $f_d = 200$ Hz. Under low Doppler shift environment, the modified LS channel estimator performs slightly better than the developed comb-type channel estimator up to an SNR of 21 dB. As the SNR increases, the difference between the performances of the estimators diminishes. Under high Doppler shift environment, both channel estimators have similar BER for SNR values up to 12 dB. As the SNR increases, the difference between the performances of the estimators increases too, and the comb-type channel estimator performs noticeably better than the modified LS channel estimator.

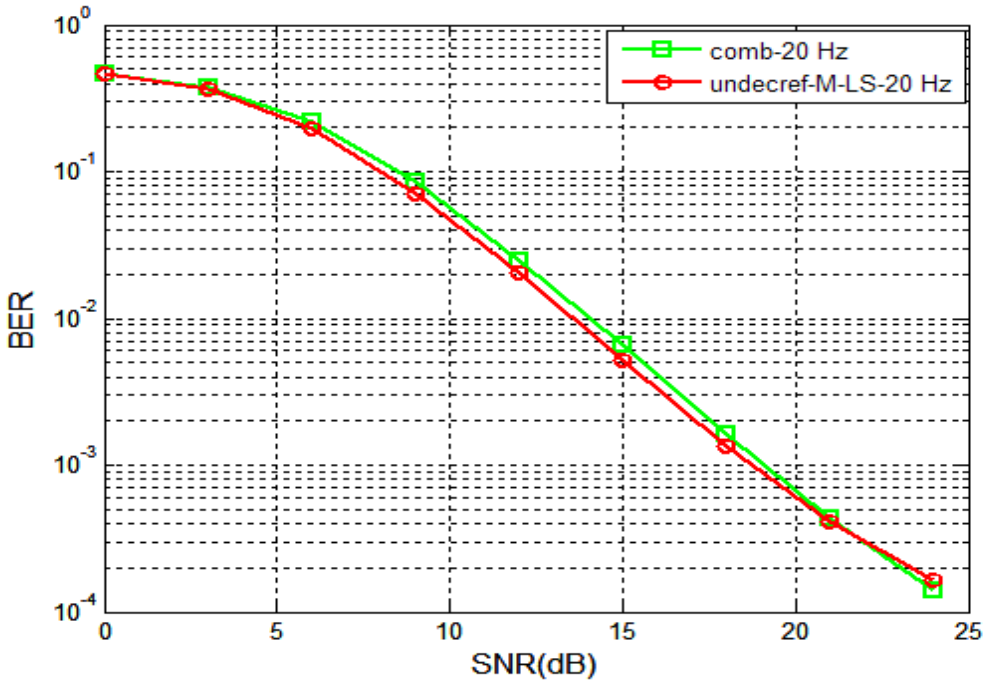

(a)

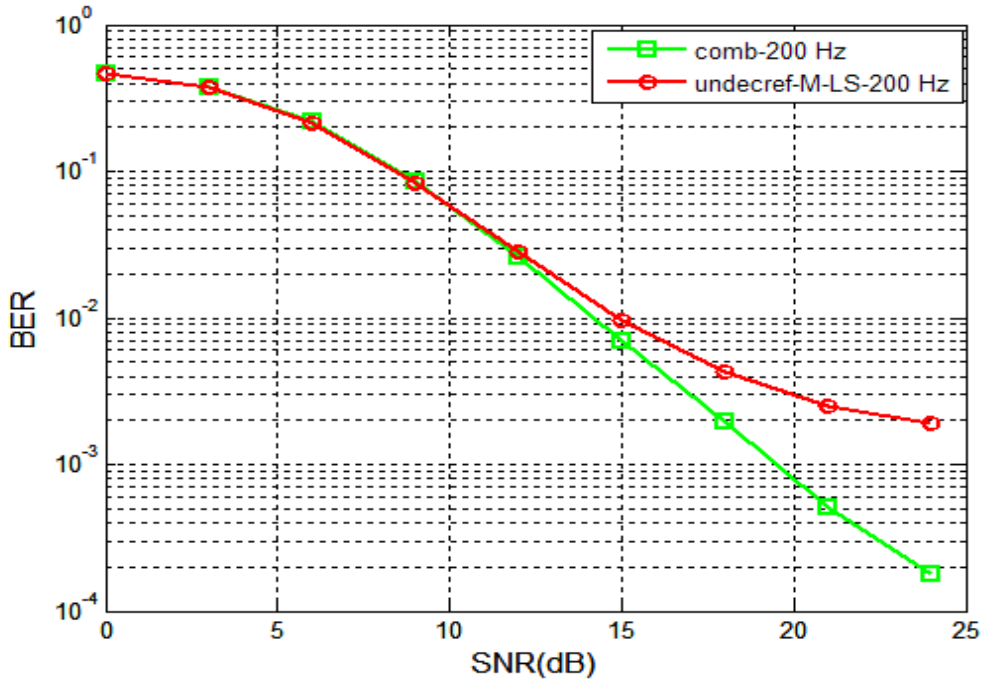

(b)

Figure 24. BER comparison of the comb-type and the modified LS channel estimators over the TU delay profile channel with (a) $f_d = 20$ Hz (b) $f_d = 200$ Hz

2. Performance of MIMO-OFDM Systems Utilizing Channel Estimation Methods

In the simulations of MIMO-OFDM (2×2) systems utilizing STBC, we used the channel estimation techniques developed in this thesis for systems with multiple transmit antennas.

As we have explained in the previous chapter, in order to generate optimum training symbols, we should not use any null sub-carriers. So, unlike the SIMO-OFDM system parameters, for the MIMO-OFDM simulations we used all of the 128 sub-channels to transmit data to be able to make a fair comparison between the basic and the simplified approaches. In most wireless standards, null sub-carriers are used to prevent interference between adjacent channels. By using no null sub-carriers, we make it easier for the channel estimator, which uses FFT operation to obtain accurate channel information since null carriers cause the estimator to lose information about those frequencies. In our simulations, this structure results in a data rate of 640 kbits/s with coding and a transmission efficiency of 0.8 bits/s/Hz including the training symbols.

In all of the simulations, we use the undecoded reference generation method in order to implement channel estimation algorithms during the data transmission period. The parameters for the simulations of the MIMO-OFDM systems are the same as the parameters given in Table 3 in Section 1 of this chapter.

Figure 25 shows the BER performance of a MIMO-OFDM system utilizing the STC estimator with a different number of taps over the TU delay profile channel with $f_d = 40$ Hz. At low SNRs, other than the estimator which uses three significant taps, all the channel estimators' performances are almost the same. With SNR higher than 10 dB, the channel estimators utilizing a greater number of taps begin to perform better. This is due to the fact that at high SNRs the estimator is able to better choose the significant taps due to the lower noise energy. For the channel model we use in our simulations, the STC estimators will lose some of the taps carrying the channel energy and this results in degradation in the channel estimator's performance. We can also see that basic channel estimator, which uses all of the 17 taps (assumed delay spread of the channel), performs better than any other STC estimator. The basic channel estimator reaches a BER of 10^{-3} at

15.5 dB, which is 1 dB worse than the perfect channel knowledge performance, and performs approximately 0.5 dB, 1.2 dB and 2.8 dB better than the basic STC estimators with fifteen, twelve and nine significant taps, respectively.

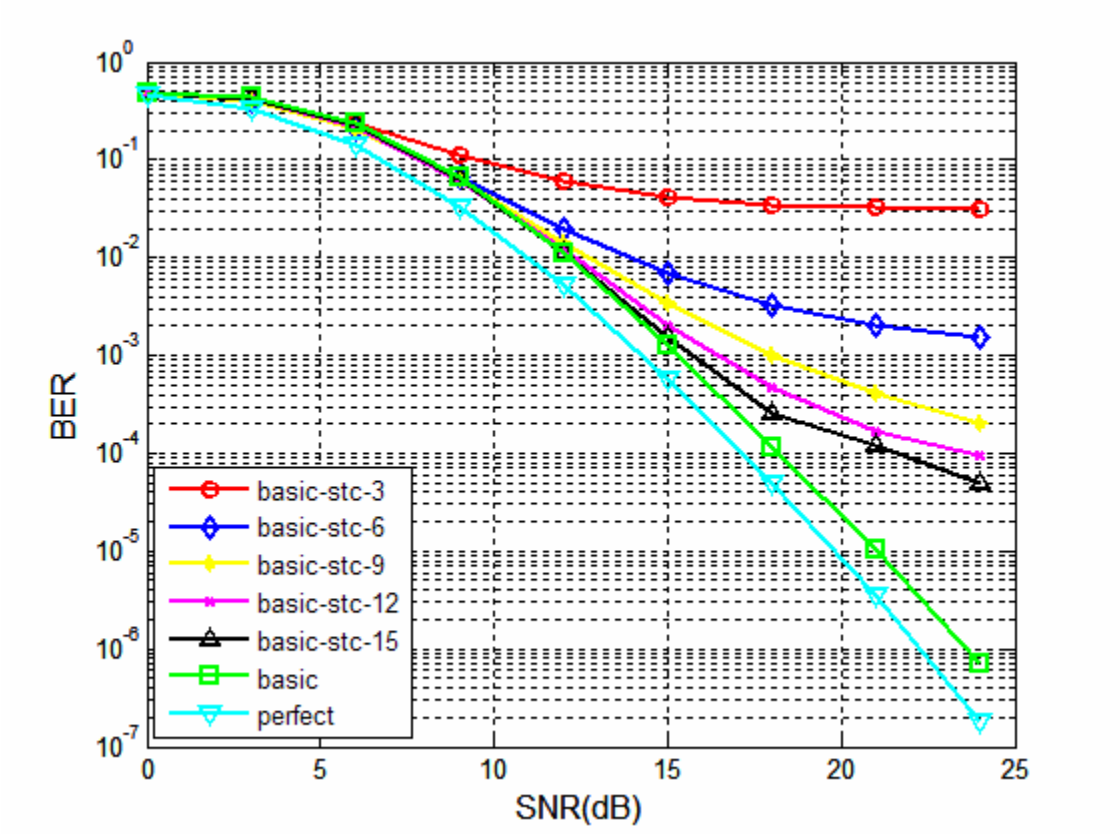

Figure 25. BER comparison of the STC estimators with different number of taps over the TU delay profile channel with $f_d = 40$ Hz

Figure 26 shows the BER performances of all of the block-type channel estimation methods examined in this thesis over the TU delay profile channel with $f_d = 40$ Hz and $f_d = 200$ Hz. For the STC estimators, we used nine taps. In both Doppler environments, the performances of the simplified channel estimators with and without STC are similar to those of the basic and the basic STC estimators', respectively. So, by using the simplified channel estimator, we get almost the same BER performance as we get with the basic channel estimator while lowering the complexity. As expected, all of the channel estimators' performances decrease while the Doppler shift of the channel increases. The basic and the simplified channel estimators reach a BER of 10^{-4} with 15.3 dB at $f_d = 40$ Hz and with 20 dB at $f_d = 200$ Hz.

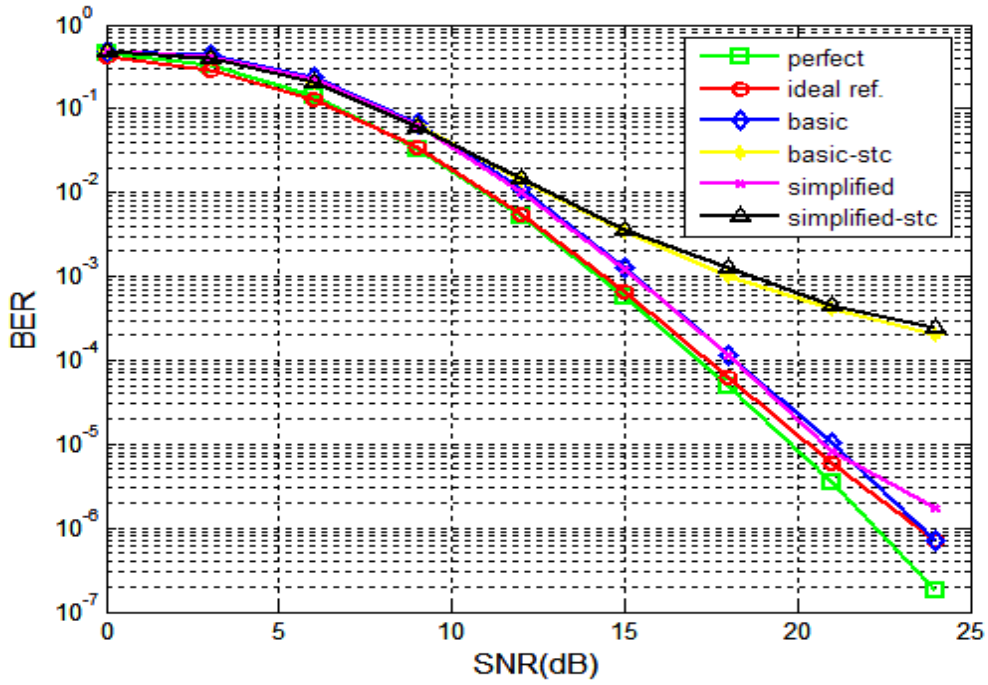

(a)

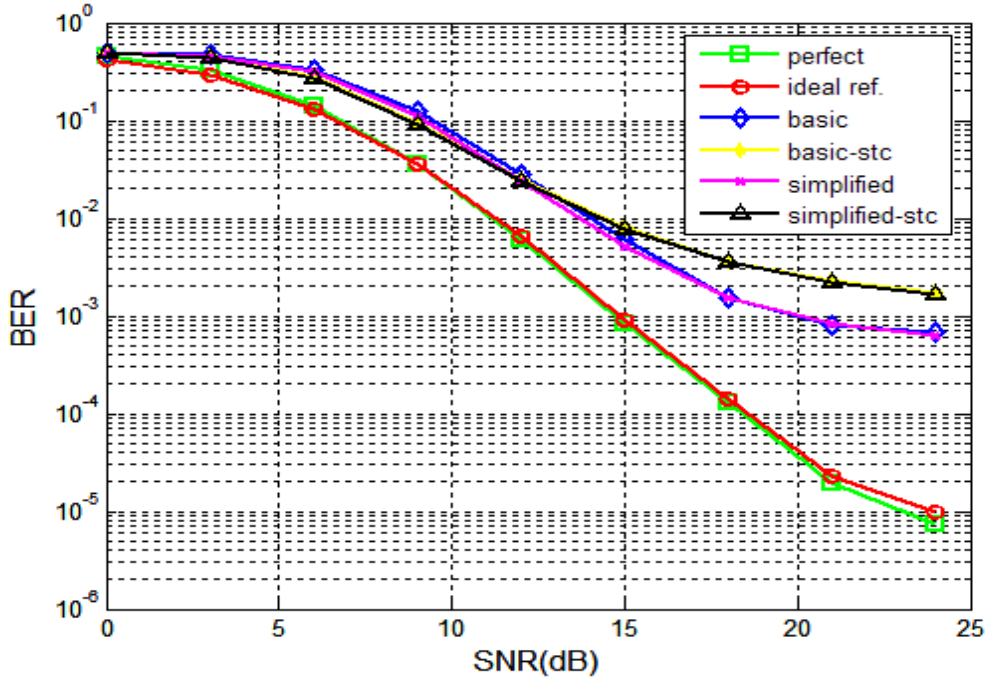

(b)

Figure 26. BER comparison of all of the block-type estimators over the TU delay profile channel with (a) $f_d = 40$ Hz (b) $f_d = 200$ Hz

Figure 27 shows the BER performance of the simplified channel estimator at various Doppler frequencies over the TU delay profile channel. The performance of the simplified estimator decays gradually as the Doppler shift of the channel increases. For the AWGN channel the simplified channel estimator reaches its best performance.

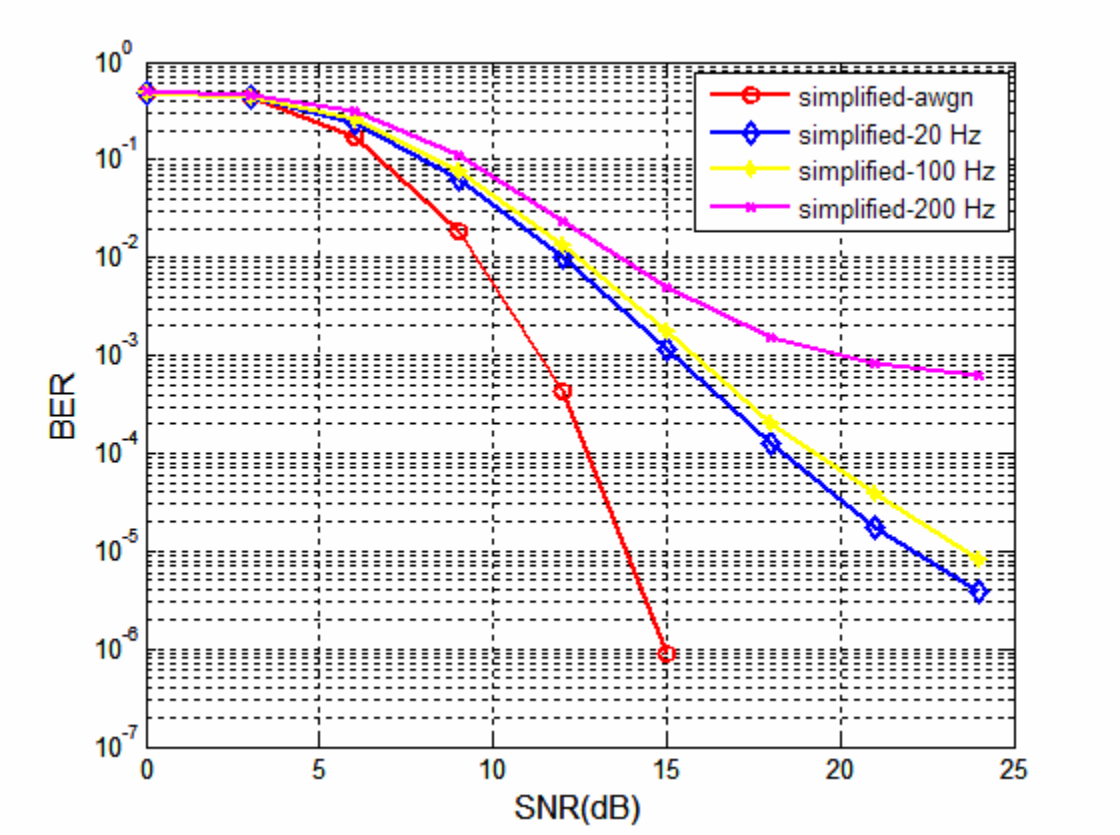

Figure 27. BER comparison of the simplified channel estimator at various Doppler frequencies over the TU delay profile channel

In order to apply the comb-type channel estimation technique to the transmitter diversity systems, the pilot insertion density we use in time and frequency is 1/4. This structure results in a 12.5% pilot symbol ratio, which is the same ratio we used for block-type channel estimation techniques for transmitter diversity systems. The pilot positions for a MIMO-OFDM system utilizing comb-type channel estimation method are chosen as $[1,5,9,...,125]$. So, we use the same simulation parameters for the comb-type channel estimation algorithm for the transmitter diversity system as shown in Table 3 in the previous section.

In Figure 28, we show the performance of the comb-type channel estimator over the TU delay profile channel with various Doppler frequencies.

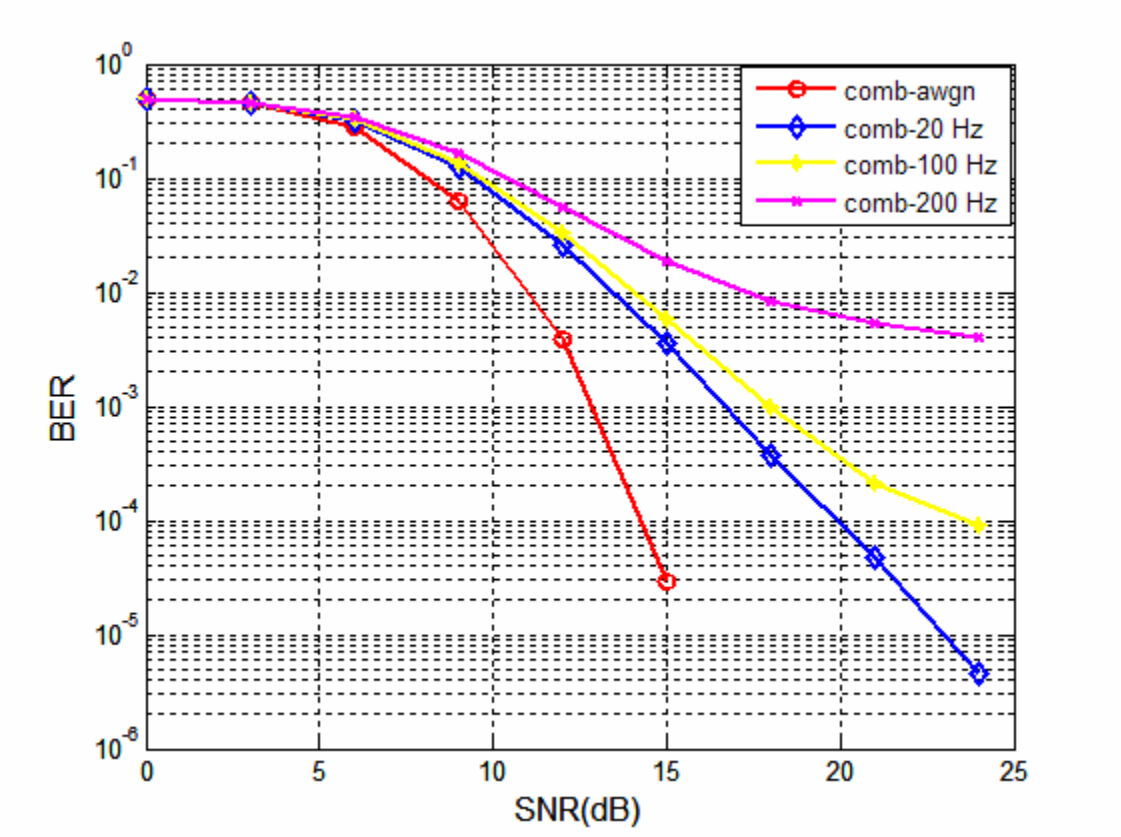

Figure 28. BER comparison of the comb-type channel estimator for transmitter diversity systems at various Doppler frequencies over the TU delay profile channel

In the SIMO-OFDM case, we have stated that the comb-type channel estimator's performance did not change significantly as the Doppler shift of the channel increased. The performance of the comb-type estimator we use for MIMO-OFDM system decreases as the Doppler frequency increases. This is due to the fact that we do not insert pilot tones in each OFDM block in order to keep the information data bandwidth efficiency at a satisfactory level. According to the pilot insertion period, we estimate the channel coefficients at every two OFDM symbol pairs and use these coefficients in the decoding operation of the following OFDM symbol pair. This results in degradation in the channel estimator's performance. We can improve the comb-type channel estimator's

performance by decreasing the pilot tone insertion period in time and frequency at the cost of reduced bandwidth efficiency.

In Figure 29, we compare the performances of both types of channel estimators over the TU delay profile channel with $f_d = 20$ Hz and $f_d = 200$ Hz.

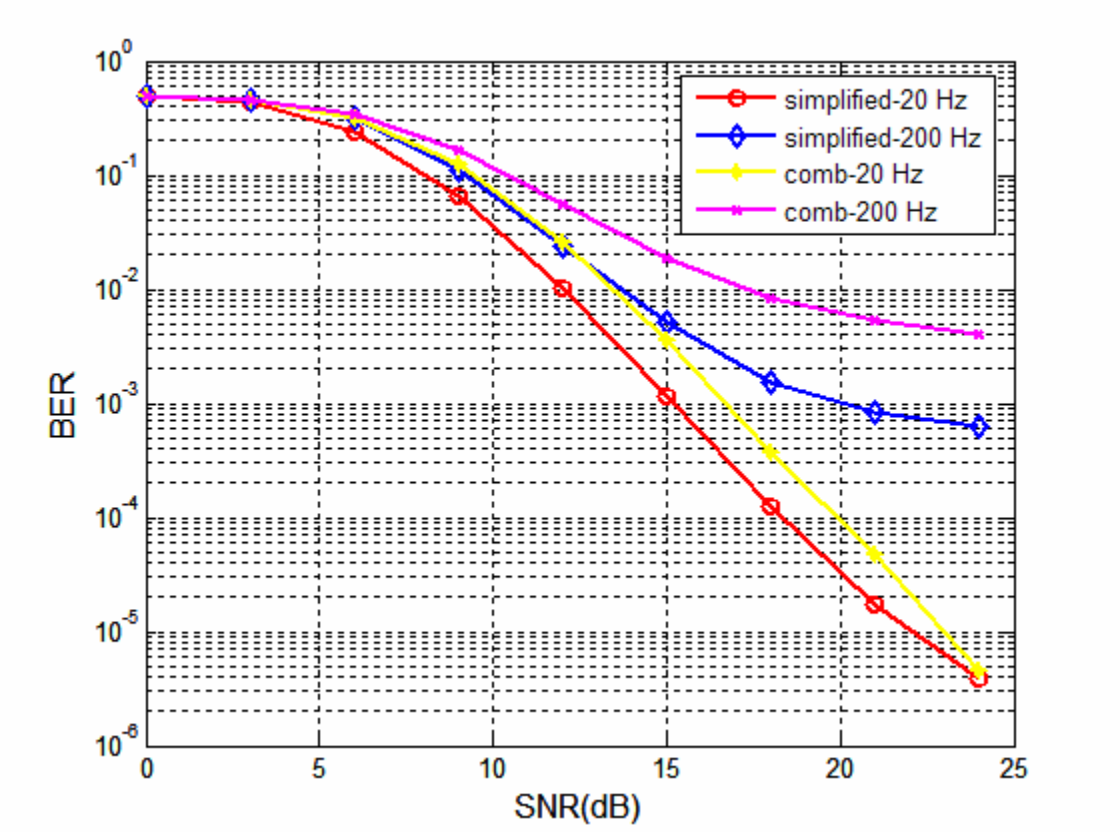

Figure 29. BER comparison of the simplified and the comb-type channel estimators at various Doppler frequencies over the TU delay profile channel

The simplified channel estimator performs better than the comb-type channel estimator under these specific circumstances. Over the channel with 20 Hz Doppler frequency, for a BER of 10^{-3}, the simplified channel estimator performs 1.5 dB better than the comb-type channel estimator and the performance difference diminishes as the SNR increases. Over the high Doppler shift channel environment, the performance difference between the channel estimators is much larger as it can be seen from Figure 29.

We show the performances of both types of channel estimators over the HT delay profile channel in Figure 30.

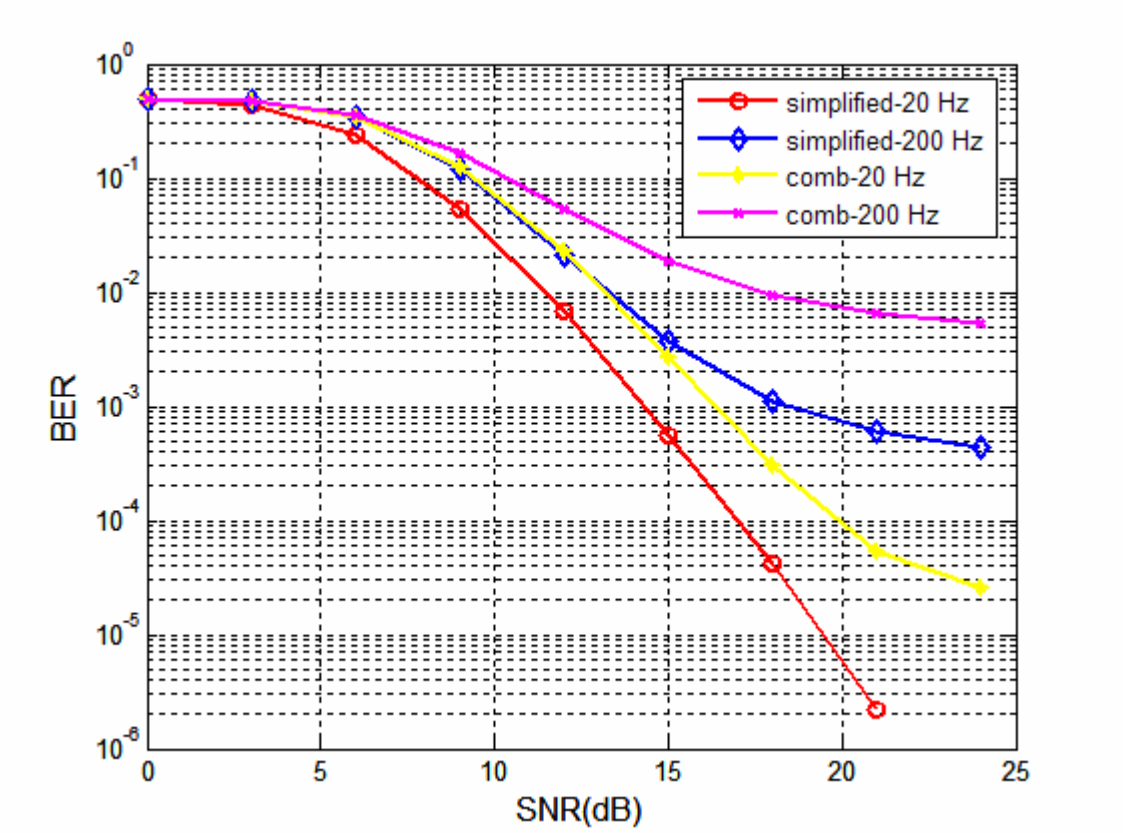

Figure 30. BER comparison of the simplified and the comb-type channel estimators at various Doppler frequencies over the HT delay profile channel

We see the same characteristics as we have seen over the TU delay profile channel. The simplified channel estimator outperforms the comb-type channel estimator at both Doppler frequencies. The simplified channel estimator's performance over the HT delay profile channel is also better than its performance over TU delay profile channel.

C. SUMMARY

In this chapter, we presented the simulation results of several Matlab-based communication systems.

First, we discussed the simulation results regarding the reference generation methods. As expected, undecoded reference generation method developed in this thesis performed better than the zero-forcing and the decoded reference generation methods and used for the following simulations. Next, the simulation results of the SIMO-OFDM

systems utilizing the LS, the modified LS and the comb-type channel estimators over the TU and the HT delay profile channels at various Doppler conditions were presented. Finally, MIMO-OFDM systems utilizing the basic, the simplified, the STC and the comb-type channel estimators' performances over the same channels were simulated and the results were discussed.

THIS PAGE INTENTIONALLY LEFT BLANK

VI. CONCLUSION

The aim of this thesis was to investigate the performances of various channel estimation techniques utilized by single and multiple-transmit antenna OFDM systems. This objective was accomplished by studying block-type and comb-type channel estimation algorithms and simulating their performances over several communication channels operating in multipath fading environments.

A. SUMMARY OF THE WORK DONE

First, we introduced MRC and STBC for single-input multiple output (SIMO) and multiple-input multiple-output (MIMO) OFDM systems. Next, a comprehensive background of channel estimation techniques for single and multiple-transmit antenna OFDM systems was presented. Finally, the effectiveness of the algorithms was assessed by computer simulations.

In the simulations, we used AWGN and discrete multipath channels to compute the BER performance curves by Monte Carlo simulations.

B. SIGNIFICANT RESULTS AND CONCLUSIONS

The simulation results were consistent with the expected behavior as presented in the current literature.

In the simulations of the SIMO-OFDM systems, we observed that the modified LS channel estimator (using only a few dominant taps of the channel) performed better than the LS channel estimator for sufficiently small SNRs. However, for higher values of the SNR, the LS channel estimator began to perform better than the modified LS channel estimator since the energy in the excluded taps became dominant compared to the channel noise.

The BER performance of the modified LS channel estimator degraded more than the performance of the comb-type channel estimator as the Doppler shift of the channel increased. This was due to the fact that the block-type channel estimator used previous blocks of data in the channel estimation process. In particular, at low Doppler frequencies (i.e., almost time invariant channels) the block-type performed better than the comb-type channel estimator while the opposite was true at high Doppler frequencies.

The basic channel estimation algorithm for the MIMO-OFDM systems requires matrix inversion. However, the simulations showed that a simplified technique that used the past values of the channel estimates seemed to work satisfactorily at any level of SNR. Using the past values of the channel estimates might cause problems, so we used a reference generation technique based on the prediction of the transmitted signal to compensate this problem. However, it should be kept in mind that in the simplified approach, we need to generate optimum training symbols and we cannot use null carriers, as mandated by a number of standards.

The STC method performed satisfactorily at low SNRs. However, at high SNRs the estimation methods based on full channel model performed significantly better.

We compared the performances of the block-type and the comb-type channel estimators also for the MIMO-OFDM systems. Unlike the SIMO-OFDM system, the performance of the MIMO-OFDM system utilizing the comb-type channel estimator degraded as the Doppler shift of the channel increased. This was due to the fact that we inserted pilots at every two OFDM symbol pairs in order to increase the bandwidth efficiency and used previously estimated channel coefficients in the decoding process of the subsequently transmitted OFDM symbol pair. Under these circumstances, the simplified channel estimation algorithm performed better than the comb-type channel estimator for any value of the Doppler frequency shift.

When the performances of the systems utilizing the developed channel estimation algorithms were compared with the performances of the systems using perfect knowledge of the channel coefficients, all simulations indicated that there was still room for improvement.

C. SUGGESTIONS FOR FUTURE STUDIES

In all simulations, we assumed that there was a perfect synchronization between the transmitter and the receiver. As a consequence, we did not take phase noise and frequency offset errors into consideration. In order to degrade the effects of lack of synchronization, frequency offset estimation and tracking must be performed. In a further study, this feature may be combined with the channel estimation algorithms developed in this thesis.

The OFDM system parameters used in this thesis were not chosen from any specific industry standard. In a future study, the developed channel estimation algorithms may be implemented with the standards, such as IEEE 802.11a or IEEE 802.16a.

Finally, the channel estimation algorithms studied in this thesis represent a specific subset of all available estimation methods, based on frequency correlation and time-domain properties of the channels. Other estimation algorithms can be found in the literature based on time correlation of the channel [3], other time-domain approaches [17] or blind channel estimation techniques [18]. These channel estimation methods may be investigated in future studies.

THIS PAGE INTENTIONALLY LEFT BLANK

APPENDIX A. MULTIPATH CHANNEL PARAMETERS

The channels which we used in our simulations are discrete multipath models specified for urban and hilly environments. These are 6-path channel models used with a TDL structure. In order to simulate differential delays correctly, we used a constant spacing TDL which uses ideal filters.

The parameters of the channels are given in Table 5. More information about the channel parameters can be found in [10].

Typical Urban (TU) Delay Profile Channel Parameters				
Tap Number	Relative Delay (μs)	Average Relative Power (dB)	Doppler Spectrum	Ricean K-Factor
1	0.0	-3.0	Jakes	0.0
2	0.2	0.0	Jakes	0.0
3	0.5	-2.0	Jakes	0.0
4	1.6	-6.0	Jakes	0.0
5	2.3	-8.0	Jakes	0.0
6	5.0	-10.0	Jakes	0.0

Hilly Terrain (HT) Delay Profile Channel Parameters				
Tap Number	Relative Delay (μs)	Average Relative Power (dB)	Doppler Spectrum	Ricean K-Factor
1	0.0	0.0	Jakes	0.0
2	0.2	-2.0	Jakes	0.0
3	0.4	-4.0	Jakes	0.0
4	0.6	-7.0	Jakes	0.0
5	15.0	-6.0	Jakes	0.0
6	17.2	-12.0	Jakes	0.0

Table 5. Parameters of the discrete multipath channels (After Ref. [10])

THIS PAGE INTENTIONALLY LEFT BLANK

APPENDIX B. MATLAB CODE EXPLANATION

In order to obtain the performances of the discussed channel estimation techniques mainly two outer functions were generated. One of these outer functions conducted the simulations for SIMO-OFDM (1×2) systems while the other one was generated for simulating MIMO-OFDM (2×2) systems.

In the outer functions, first we generate the channel coefficients and the OFDM symbols to be transmitted. After the transmission at the baseband level, we perform the signal reception and the channel estimation processes. Lastly, decoding operation and BER computation are conducted.

There are mainly three iterations as Monte Carlo, SNR and bit iterations. For the simulations where we measured the performances of the systems at several Doppler frequencies, we also added Doppler iteration to the outer functions.

Some of the functions used in the Matlab code are taken from [13]. Here, we explain the functions generated for simulating the communication systems.

estimation_simo.m is the outer function which simulates a SIMO-OFDM system utilizing the LS, modified LS and the comb-type channel estimators. It generates the BER and the normalized MSE curves as the result.

estimation_mimo.m is the outer function which simulates a MIMO-OFDM system utilizing the basic, the simplified, the STC and the comb-type channel estimators. It generates the same curves as *estimation_simo.m* does.

create_simo_ch.m is used to generate the channel coefficients for a 1×2 OFDM system. The channel delay profile to be used can be chosen here. It produces the coefficients of two channels. It calls *jakes.m* in order to perform the spectrum shaping of the coefficients. It produces K_0 taps which represent the impulse response of the channel and gives as many impulse responses as the number of OFDM blocks to be transmitted as the output.

create_mimo_ch.m is used to generate the channel coefficients for a 2×2 OFDM system. Unlike *create_simo_ch.m*, it produces coefficients for four channels totally.

jakes.m is the function which generates the complex Gaussian white noise processes and applies the Jakes spectrum to them.

opt_trn.m generates the optimum training symbols used in MIMO-OFDM systems. This is essential for simplified channel estimation method especially. Optimum training symbols are produced once and the same symbols are used for all training symbol transmissions.

sym_gen.m is the function which generates all the OFDM blocks to be transmitted. For MIMO-OFDM systems, optimum training blocks are inserted at the training block transmission positions. Since we do not use any special training symbols for the SIMO-OFDM systems, all the OFDM symbols are generated in this function. The information bits to be transmitted are generated by using a random number generator and passed through the convolutional encoder. The coded bits are then digitally modulated and mapped to m-ary symbols. It calls *bin_2_mary.m* and *ifft_128.m*.

sym_gen_comb.m generates the OFDM symbols to be transmitted for the MIMO-OFDM systems utilizing comb-type channel estimation technique. We need to use specially generated pilot symbols inserted between the data symbols for the comb-type channel estimation algorithm and this is the reason why we built a separate symbol generator. First, the information bits are generated, convolutionaly coded and mapped to symbols. Subsequently, the pilot tones are inserted between these information symbols. It calls *pilot_ins.m* other than the *bin_2_mary.m* and *ifft_128.m*.

bin_2_mary.m converts the convolutionaly encoded bits to m-ary symbols. The output of this function is a vector with decimal numbers representing the symbols in the m-ary constellation diagram.

ifft_128.m is the function which applies 128-point IFFT and adds the guard interval to the input complex sequence. For SIMO-OFDM systems, it also adds the null sub-carriers at the edges.

pilot_ins.m generates the special pilots to be used for the systems utilizing the comb-type channel estimation.

add_noise.m is the function which generates the AWGN sequence to be added to

the received signals. The variance of the noise is determined from the received signals' power and the SNR value used at that time.

fft_128.m takes the noise added received OFDM block, removes the guard interval and applies 128-point FFT.

est_ch_fre_res.m performs channel estimation for the SIMO-OFDM systems which use LS and modified LS channel estimation algorithms. At the output, it gives the frequency responses of the estimated channels.

est_ch_infoc.m selects the frequency response part of the channel corresponding to information sub-carriers.

est_comb.m performs the channel estimation for the systems which use the comb-type channel estimator. At the output, it gives the frequency responses of the channels corresponding to information sub-carriers.

est_ch_basic.m is the function which performs the basic channel estimation. Basic STC method can also be chosen. There are two different algorithms written to be used with either optimum training symbols or with any other training symbols in this function. At the output, it gives the frequency responses of the channels.

est_ch_simp.m performs the simplified and the simplified STC channel estimation methods. At the output, it gives the frequency responses of the channels.

se_nmse.m computes the square error between the estimated and the ideal channel frequency responses.

comparator.m performs the demapping, decoding and the bit comparison operations for the systems which use block-type channel estimation techniques. At the output, it gives the number of bit errors for the received OFDM symbol. It calls *mary_2_bin.m*.

comparator_comb.m performs the same operations as *comparator.m* does but for the systems which use comb-type channel estimation algorithm. It calls *mary_2_bin.m* and *pilot_ejt.m* in order to obtain the sequence which only consists of information symbols. The output is the number of bit errors for the received OFDM symbol.

mary_2_bin converts the decimal numbers to bits by using the chosen constellation diagram.

pilot_ejt.m removes the pilot symbols from the received OFDM symbol and gives the received information symbols as the output.

nmse_mean.m computes the average MSE of all the channels at each SNR value.

LIST OF REFERENCES

[1] S. M. Alamouti, "A Simple Transmit Diversity Technique for Wireless Communications," *IEEE Journal on Selected Areas in Communications*, Vol. 16, No. 8, pp. 1451-1458, October 1998.

[2] E. Lindskog and A. Paulraj, "A Transmit Diversity Scheme for Channels with Intersymbol Interference," *Proceedings of IEEE International Conference on Communications, 2000*, Vol. 1, pp. 307-311, June 18, 2000.

[3] Y. Li, J. Cimini, Jr., and N. R. Sollenberger, "Robust Channel Estimation for OFDM Systems with Rapid Dispersive Fading Channels," *IEEE Transactions on Communications*, Vol. 46, No. 7, pp. 902-915, July 1998.

[4] J. G. Proakis, *Digital Communications*, pp. 822-823, McGraw Hill, New York, 2001.

[5] J. -J. van de Beek, O. Edfords, M. Sandell, S. K. Wilson, and P. O. Börjesson, "On Channel Estimation in OFDM Systems," in *Proc. 45th IEEE Vehicular Technology Conf.*, pp. 815-819, Chicago, IL, July 1995.

[6] S. Coleri, M. Ergen, A. Puri and A. Bahai, "Channel Estimation Techniques Based on Pilot Arrangement in OFDM Systems," *IEEE Transactions on Broadcasting*, Vol. 48, pp. 223-229, September 2002.

[7] Y. Li, N. Seshadri, and S. Ariyavisitakul, "Channel Estimation for OFDM Systems with Transmitter Diversity in Mobile Wireless Channels," *IEEE Journal on Selected Areas in Communications*, Vol. 17, No. 3, pp. 461-471, March 1999.

[8] B. Song, Y. Guan and W. Zhang, "An Efficient Training Sequences Strategy for Channel Estimation in OFDM Systems with Transmit Diversity," *Journal of Zhejiang University Science*, pp. 613-618, Institute of Image Communication and Information Processing, Shanghai Jiaotong University, Shanghai 200030, China, 2005.

[9] Y. Li, "Simplified Channel Estimation for OFDM Systems with Multiple Transmit Antennas," *IEEE Transactions on Wireless Communications*, Vol. 1, No. 1, pp. 67-75, January 2002.

[10] Michel C. Jeruchim, Philip Balaban and K. Sam Shanmugan, *Simulation of Communication Systems*, pp. 545-621, Kluwer Academic / Plenum Publishers, New York, 2000.

[11] Mary Ann Ingram, "Tutorial for Multipath," Smart Antenna Research Laboratory, http://users.ece.gatech.edu/~mai/tutorial_multipath.htm, last accessed 21 June 2005.

[12] W.C. Jakes, *Microwave Mobile Communications*, Wiley, New York, 1974.

[13] H. D. Saglam, *Simulation Performance of Multiple-Input Multiple-Output Systems Employing Single-Carrier Modulation and Orthogonal Frequency Division Multiplexing*, Master's Thesis, Naval Postgraduate School, Monterey, California, December 2004.

[14] Institute of Electrical and Electronics, 802.11a, *Wireless LAN Medium Access Control (MAC) and Physical Layer (PHY) Specifications: High-Speed Physical Layer Extension in the 5 GHz Band*, 16 September 1999, http://ieeexplore.ieee.org, last accessed 21 June 2005.

[15] S. B. Weinstein and P. M. Ebert, "Data Transmission by Frequency-Division Multiplexing Using the Discrete Fourier Transform," *IEEE Transactions on Communications*, Vol. 19, No. 5, pp. 628-634, October 1971.

[16] R. Negi and J. Cioffi, "Pilot Tone Selection for Channel Estimation in a Mobile OFDM System," *IEEE Transactions on Consumer Electronics*, Vol. 44, No. 3, pp. 1122-1128, August 1998.

[17] H. Minn and V. K. Bhargava, "An investigation into Time-Domain Approach for OFDM Channel Estimation," *IEEE Transactions on Broadcasting*, Vol. 46, No. 4, pp. 240-248, December 2000.

[18] A. Petropulu, R. Zhang and R. Lin, "Blind Channel Estimation through Simple Linear Precoding," *IEEE Transactions on Wireless Communications*, Vol. 3, No. 2, pp. 647-655, March 2004.

INITIAL DISTRIBUTION LIST

1. Defense Technical Information Center
   Ft. Belvoir, Virginia

2. Dudley Knox Library
   Naval Postgraduate School
   Monterey, California

3. Chairman, Code EC
   Department of Electrical and Computer Engineering
   Naval Postgraduate School
   Monterey, California

4. Professor Roberto Cristi, Code EC/Cx
   Department of Electrical and Computer Engineering
   Naval Postgraduate School
   Monterey, California

5. Professor Murali Tummala, Code EC/Tu
   Department of Electrical and Computer Engineering
   Naval Postgraduate School
   Monterey, California

6. Halil Derya Saglam
   Koru Mah. 499.Sok. No=I/2, Birlikkent Sitesi
   Cayyolu, Ankara, TURKEY

7. Mumtaz Bilgin Sen
   Pasabayir Mah. Sofuoglu Cad. Dostlar Sit. A/3
   Bandirma, Balikesir, TURKEY